UCRL-53673

Estimates of *In Situ* Deformability with an NX Borehole Jack, Spent Fuel Test—Climax, Nevada Test Site

W. C. Patrick

J. L. Yow, Jr.

M. C. Axelrod

December 1985

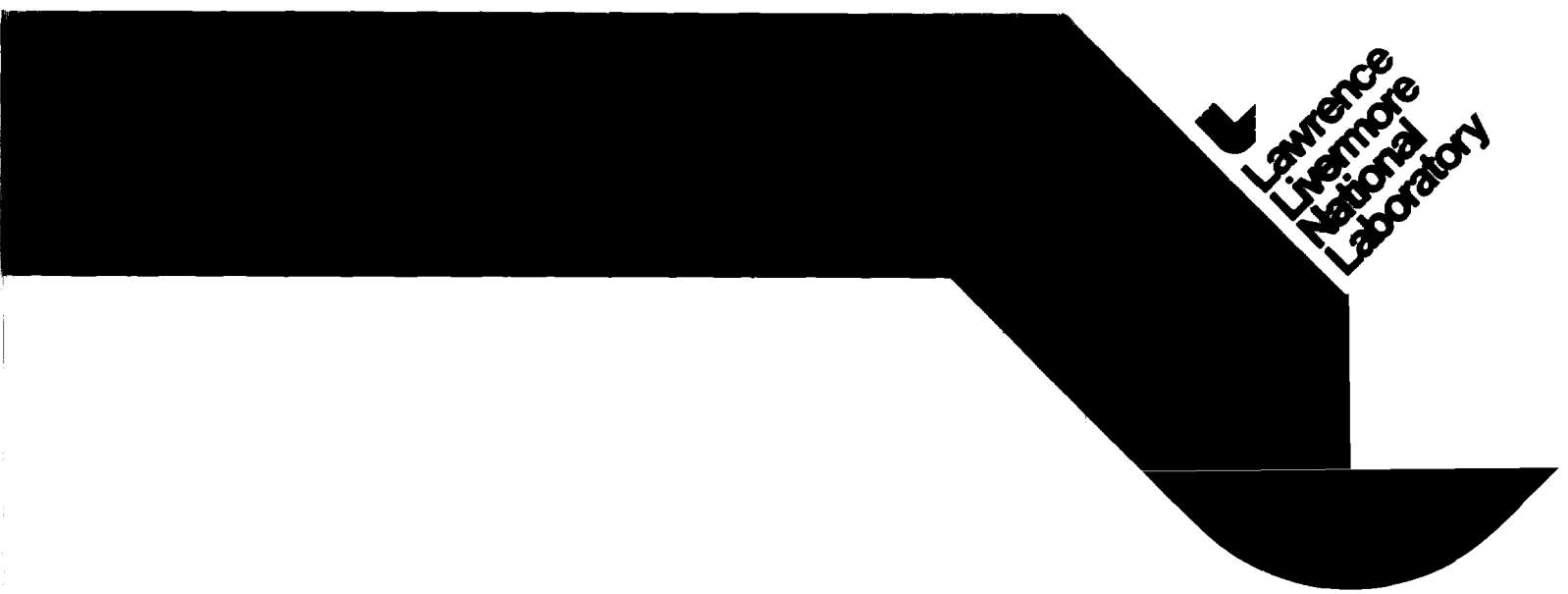

Work performed under the auspices of the U.S. Department of Energy by Lawrence Livermore National Laboratory under Contract W-7405-ENG-48.

UCRL-53673
Distribution Category UC-70

Estimates of *In Situ* Deformability with an NX Borehole Jack, Spent Fuel Test—Climax, Nevada Test Site

W. C. Patrick

J. L. Yow, Jr.

M. C. Axelrod

Manuscript date: December 1985

LAWRENCE LIVERMORE NATIONAL LABORATORY
University of California • Livermore, California • 94550

Available from: National Technical Information Service • U.S. Department of Commerce
5285 Port Royal Road • Springfield, VA 22161 • A02 • (Microfiche A01)

Contents

Estimates of *In Situ* Deformability with an NX Borehole Jack, Spent Fuel Test—Climax, Nevada Test Site*

Abstract

A series of borehole modulus measurements was obtained at the Spent Fuel Test—Climax (SFT—C) facility following removal of heat sources and a subsequent 1-year cooling period. A total of 212 measurements were obtained using a standard hardrock NX borehole (Goodman) jack. The results of 64 measurements made at the site before heating were reanalyzed for comparison with the post-heat data. Modulus values were calculated from the straight-line portion of the pressure vs displacement curves.

Although the deformation modulus was observed to be highly variable, models were developed to explain much of this variability. Typically, spacial effects, anisotropy, and heating effects were present. The test results indicate that the deformation modulus tended to increase in the pillars between the underground openings where temperatures increased about 10°C above the ambient 24°C during the SFT—C. Conversely, a decrease in modulus was observed where temperatures were near 60°C for a three-year period. In most cases, we found the modulus values to be slightly higher for vertical than for horizontal loading. There was a tendency for the modulus to be lower near excavated openings. While this effect was not ubiquitous, it was statistically significant.

Introduction and Background

The Spent Fuel Test—Climax (SFT—C) is a test of deep geologic storage and retrieval of commercial spent nuclear fuel assemblies (Ramspott et al., 1979). Conducted under the technical direction of the Lawrence Livermore National Laboratory (LLNL), the test is part of the Nevada Nuclear Waste Storage Investigations, which are administered by the Department of Energy's Nevada Operations Office.

The basic geometry of the SFT—C facility is three parallel drifts connected at their ends (Fig. 1). The center drift is 6.1 m high × 4.6 m wide × 65 m long and has 17 storage boreholes in the floor, which held 11 spent nuclear fuel assemblies and 6 electrical heaters during the 3-year heated phase of the test. Parallel heater drifts measuring 3.4 m × 3.4 m in section are located on either side of the center drift. Each of these heater drifts had 10 electrical heaters located in the floor during the 3-year heated phase of the test. This combination of heat and radiation sources simulated the thermal effects of a panel of a full-scale repository, raising rock temperatures to 85°C near the storage boreholes in the center drift and to well over 300°C near the electrical heaters in the two side drifts (Patrick et al., 1982 and 1983).

Rock deformability characteristics are required for input to calculations of displacements and stress changes that would occur as a result of excavating and later heating the SFT—C facility. Several laboratory studies were conducted to determine the Young's modulus and Poisson's ratio of intact cores of the Climax stock quartz monzonite (CSQM) in which the test facility is located

* Prepared by Nevada Nuclear Waste Storage Investigations (NNWSI) Project participants as part of the Civilian Radioactive Waste Management Program. The NNWSI Project is managed by the Waste Management Project Office of the U.S. Department of Energy, Nevada Operations Office. NNWSI Project work is sponsored by the Office of Geologic Repositories of the Department of Energy Office of Civilian Radioactive Waste Management.

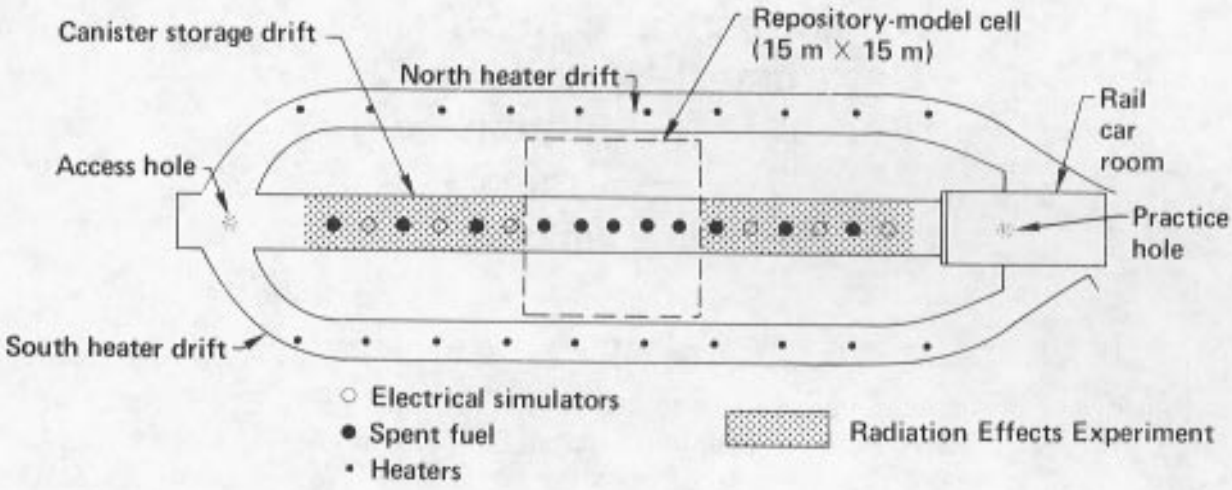

Figure 1. Plan view of Spent Fuel Test—Climax facility showing location of thermal sources and principal experiments.

(Table 1). Since the rock mass was known to be moderately to heavily fractured, *in situ* determination of the deformation characteristics was necessary on a somewhat larger scale than could be readily performed in the laboratory.

Before the heated phase of the test began, Heuze et al. (1981) estimated the *in situ* deformation characteristics using several techniques, including the Goodman NX borehole jack (Table 1). A total of 64 borehole jack measurements was

Table 1. Summary of deformation characteristics of Climax stock quartz monzonite.

Specimen size	Test conditions	Young's modulus (GPa)	Poisson's ratio	Source
76-mm-diam (NX) core	Uniaxial compression	61.4–69.7	0.21–0.22	Maldonado, 1977
76-mm-diam (NX) core	Uniaxial compression	48 ± 5	0.21 ± 0.02	Pratt et al., 1979
76-mm-diam (NX) core	Uniaxial compression	51 ± 5	0.22 ± 0.02	Pratt et al., 1979
	Triaxial compression,			
143-mm-diam core	σ_3 = 3.4 MPa	66.7 ± 5.9	0.35 ± 0.02	Pratt et al., 1979
143-mm-diam core	σ_3 = 6.9 MPa	54.4 ± 5.1	0.27 ± 0.06	Pratt et al., 1979
143-mm-diam core	σ_3 = 10.3 MPa	61.8 ± 7.0	0.31 ± 0.05	Pratt et al., 1979
143-mm-diam core	σ_3 = 20.7 MPa	63.7 ± 6.4	0.31 ± 0.05	Pratt et al., 1979
143-mm-diam core	σ_3 = 41.4 MPa	66.8 ± 1.9	0.28 ± 0.05	Pratt et al., 1979
143-mm-diam core with EX center hole	Biaxial compression (USBM gauge)	68.3 ± 6.2	N/M[a]	Creveling et al., 1984
143-mm-diam core with EX center hole	Biaxial compression (CSIRO cell)	70.3 ± 3.4	0.29 ± 0.02	Creveling et al., 1984
N/A[b]	NX jack	20–30	N/M	Heuze et al., 1981
N/A	Modified NX jack	50–80	N/M	Heuze et al., 1981
N/A	Petite sismique	47–52	N/M	Heuze et al., 1981
N/A	Tunnel relaxation	20–32	N/M	Heuze et al., 1981
N/A	RMR-rating	20–31	N/M	Heuze et al., 1981
N/A	Q-System rating	10–37	N/M	Heuze et al., 1981

[a] N/M = Not measured.
[b] N/A = Not applicable.

made in alternating vertical and horizontal loading directions. These tests were conducted in four horizontal borehole segments located in the pillars between the three drifts while the rock mass was at ambient temperature (~24°C).

While the best estimate for the laboratory modulus was reported as 70 GPa, the estimate for the field deformation modulus was reported as 26 GPa. The modulus reduction factor of 0.37 was judged to be consistent with those observed by other researchers, as summarized by Heuze et al. (1981).

The impetus for the study reported here was the need to determine what changes had occurred in large-scale deformability characteristics as a result of elevating the temperature of the SFT—C facility, and to determine the deformability outward from the excavations. Thermally induced changes in deformability could result in discrepancies between displacements and stress changes that were calculated to occur and those that were actually measured during the SFT—C. Therefore, observed changes would be applied to a series of revised displacement and stress calculations. As a result of post-heating geologic sampling activities at the site, additional NX boreholes were available for this study. These new boreholes permitted evaluation of the effects of heating over a broader temperature range than would have been possible using only data from the pillar boreholes. In addition, they provided data for a more thorough analysis of anisotropy of the *in situ* deformation modulus.

Geological Setting

The SFT—C is located 420 m below ground surface in the quartz monzonite unit of a two-part intrusive. The test level is about 150 m above the regional water table and is unsaturated but not dry. The Climax stock quartz monzonite is a light-to-medium-gray porphyritic rock with large pink alkali feldspar phenocrysts scattered throughout the groundmass. The phenocrysts are up to 150 mm long and are in a groundmass consisting of 0.25- to 5-mm quartz grains, 0.25- to 3.5-mm plagioclase grains, and 1.5-mm biotite grains (Connolly, 1981).

Wilder and Yow (1984) report four dominant joint sets and three much less prominent sets in the test area (Table 2). The rock mass is moderately jointed with frequencies ranging from 0.90 joints/m to 2.2 joints/m (Table 3). Of more direct interest for this study is the frequency of joints perpendicular (or nearly so) to the test loading directions. Table 3 displays this information. Joints observed in a borehole oriented at N61°W, for example, would have the most effect on modulus measurements where the loading direction was N61°W. The "open joints" referred to here include both clean and infilled fractures, as distinguished from "healed joints." As reported by Wilder and Yow (1984), the latter are in general thoroughly healed with quartz and, while some pyrite and sericite may be present, are thought to be nearly as strong and stiff as the rock mass.

Since a borehole does not sample the most significant fractures (those perpendicular to the loading direction of the modulus tests conducted in that borehole), individual borehole fracture logs are not presented here.

In addition to the systematic joint sets, shear and fault zones also intersect the SFT—C facility. Figure 2 indicates the location of shears and faults in plan view, together with the more systematic joints. Note the proximity of these geological features with respect to the boreholes in which deformability measurements were made.

Table 2. Dominant joint sets in the vicinity of the SFT—C facility (after Wilder and Yow, 1984).

Strike	Dip	Fractional percentage of total number of joints observed (n = 1557)
N44°W	20°NE	23
N24°W	Vertical	23
N59°W	Vertical	35
N48°E	80°SE	12
Three less-dominant sets combined		7

Table 3. Fracture frequencies and spacings associated with borehole orientations.

Data source	Borehole orientation	Mean frequency of open joints (joints per m)	Mean fracture spacing of open joints (m)
UG01	N61°W, horizontal	2.00	0.50
MBI07 and 14	N29°E, horizontal	2.20	0.45
G × E	Vertical downward	1.87	0.53
UG02	N61°W, 60° below horizontal	1.50	0.67
BMT01 and 02	N29°E, horizontal	0.92	1.08
NHH10A	Vertical downward	1.83	0.55
SHH05A	Vertical downward	0.90	1.11

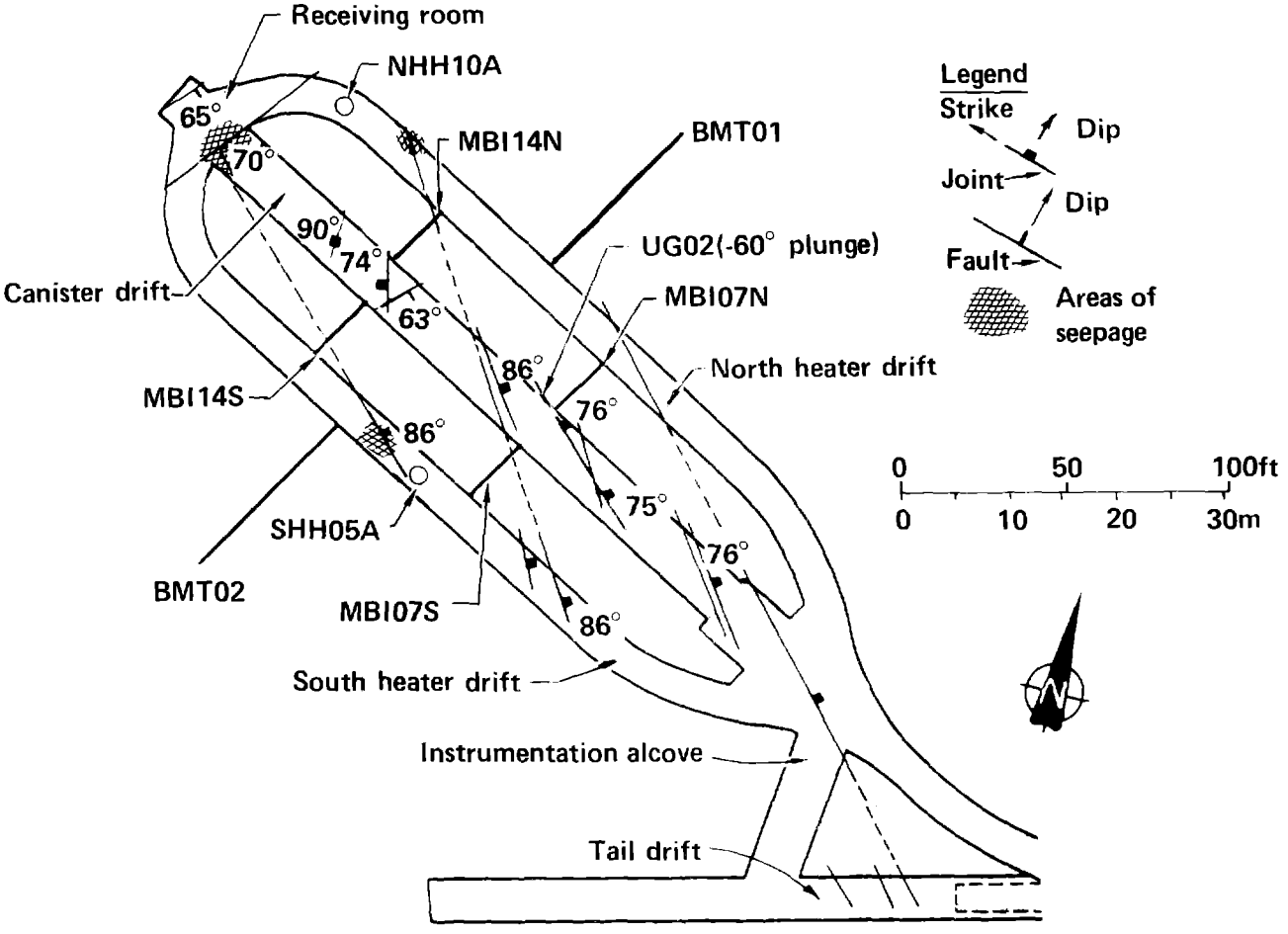

Figure 2. Major geologic features and water seepage locations.

Experimental Setting

Boreholes for deformation modulus measurements were positioned based on two criteria (Fig. 2). First, several NX boreholes were required for preheat exploration of the test area (borehole UG02), for installation of displacement instrumentation (boreholes MBI07 and MBI14, referred to as IMB07 and IMB14 when discussed in conjunction with preheat modulus data), and for post-heat geological sampling (boreholes NHH10A and SHH05A). The locations and orientations of these boreholes were determined based on the primary purpose of the borehole rather than their specific merits for deformability measurements. Second, two boreholes (BMT01 and BMT02) were located and oriented specifically to obtain deformability data outward from the SFT—C facility.

Two different bit types were used to core the test boreholes. The UG- and MBI-series boreholes were drilled in 1979, during development of the SFT—C facility, using standard surface-set NX diamond bits. Because a reamed hole was not required by the primary purpose of the borehole, no reaming shell was used in this drilling activity. As a result, the boreholes tend to be undersized as much as 1.52 mm (0.060 in.). The post-heat drilling of BMT01, BMT02, SHH05A, and NHH10A used composition diamond bits that produced a somewhat larger diameter borehole. Once again, no reaming shell was used. These boreholes tend to be oversized as much as 1.52 mm (0.060 in.). The frequency histogram of deviations in borehole diameter shows a distinct bimodal shape that is a direct result of using the two bit types (Fig. 3). All boreholes were flushed initially with water to remove drill cuttings and subsequently with compressed air to remove excess water.

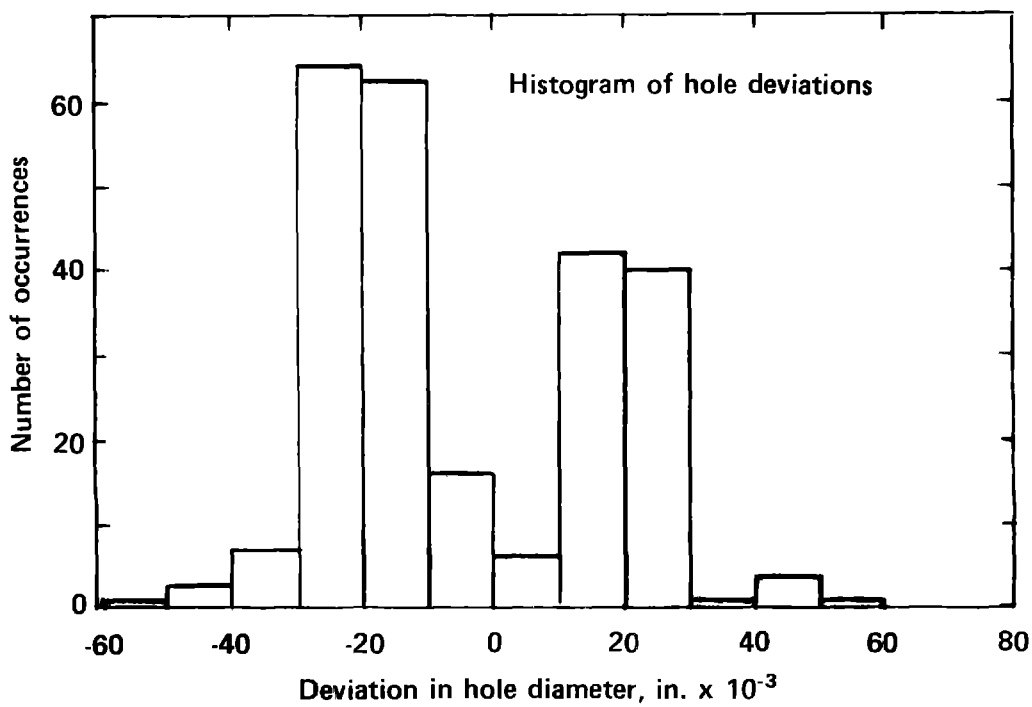

Figure 3. Histogram of deviations in borehole diameters at locations where pre- and post-test modulus measurements were made.

Measurement Procedure

Using conventional NX borehole jack equipment, jack pressure and displacement data were obtained at selected borehole depths in two orthogonal directions. The equipment consisted of a Slope Indicator Co. Model 52101 hardrock borehole jack, a 69-MPa (10,000-psi) hydraulic pump with pressure gauge, a two-channel linear variable differential transformer (LVDT) readout box, and associated hydraulic and electrical cables and connections. Although measurements in the MBI-series boreholes used the same serial number borehole jack as was leased from Slope Indicator Co., Seattle, Washington, and used by Heuze et al. (1981), a complete set of equipment was purchased to conduct the rest of the tests for this study. All equipment was calibrated by the manufacturer or LLNL, as appropriate.

Test depths were selected to correspond to the locations of earlier tests performed by Heuze in MBI07 and MBI14, and to provide a sufficiently dense data set to discern spacial variations in deformability in BMT01, BMT02, NHH10A, SHH05A, and UG02. Although loading orientations in horizontal boreholes were vertical and transversely horizontal (N61°W), loading orientations in vertical boreholes and in borehole UG02 were parallel (N61°W) and perpendicular (N29°E) to the drift centerlines.

Test depths and orientations were established by making scribe marks on the BX drill casing that was used to insert the jack into the borehole. A tape measure was used to determine to the nearest centimeter the depth from the jack centerline to a reference point on the drift wall or floor.

Table 4. Test procedures used in the current study compared with ASTM suggested method (Heuze, 1984).

Procedure for this study	ASTM suggested method	Comment
1. Prequalify test personnel	Same	Standard QA practice
2. Calibrate equipment	Same	Standard QA practice
3. One rock type tested	Test each rock type at site including fracture and alteration zones	Attempted to test fault zone but hole was too irregular and oversized
4. Conduct test in different orientations	Same	Measurements in three orthogonal directions
5. Sufficient tests for statistical analysis	Same	212 tests in 9 borehole segments
6. Holes not reamed, calibrated jack readings used as caliper	Ream boreholes to 76.2 mm	See "Experimental Setting"
7. Holes cored and logged	Same	Did not use oriented core
8. Systematic but arbitrary spacing used	Select test locations based on borehole log; test discontinuities	Net effect was the same in this jointed rock
9. Standard equipment used	Standard manufacturer's equipment plus casing alignment tool	A different technique was used to scribe casing (see text above)
10. Clean boreholes with water	Same	Standard practice
11. Seating pressure of 345 to 790 kPa used except for MBI07 and 14	Seating pressure of 345 kPa	Nominally zero seating pressure in MBI07 and 14 for consistency with preprevious study
12. Test to maximum jack capacity	Same, monitor time-dependent deformation for 15 min	69-MPa line pressure (peak jack pressure) held for minimum of 2 min, some tests held for over 30 min with no observable change in displacements
13. Alternating tests cycled twice to 100% of jack capacity, 6.9-MPa increments	25% of tests to evaluate effects of cycling to 30, 60, and 100% of maximum in 10 increments	Field evaluations showed no cyclic behavior in sample tests
14. Tests at two orientations performed at same depth	Move jack 30.5 cm between tests of different orientations	Needed a high data density, macrofracturing of rock unlikely at these stresses
15. Record data on standard format	Same	Standard QA practice

Angular orientations were established by eye, using scribe marks referenced to vertical, horizontal, parallel, or perpendicular to the drift, as appropriate. Orientations are correct to within about 5°. In some cases it was necessary to change the depth of a test because differences between readings of the near and far LVDTs exceeded 0.508 mm (0.020 in.). The manufacturer suggests that differences much larger than this should be avoided to prevent possible damage to the jack. This suggested limit was exceeded in only 11 of 212 cases, and in only 4 cases was the limit exceeded by more than 0.127 mm (0.005 in.).

Although a recently suggested method for using the NX borehole jack was not available at the time these tests were conducted, it is informative to compare the procedures used in this study with the suggested method (Heuze, 1984). Table 4 summarizes this comparison. The borehole diameter was established by the average of the jack LVDT readings at the nominal 0.3- to 0.8-MPa seating pressure. The calibrated jack was used in this manner to caliper the borehole at the location of each measurement.

Method of Analysis

The fundamental method of analysis was that suggested by Heuze (1984). The calculated deformation modulus is

$$E_c = 0.86 \cdot 0.93 \cdot D \cdot \frac{\Delta Q_h}{\Delta D} \cdot T^* \quad , \qquad (1)$$

where

- E_c is the calculated deformation modulus in psi,
- 0.86 is a calculated factor accounting for three-dimensional effects,
- 0.93 is the efficiency of the hydraulic system,
- D is the initial borehole diameter, taken as 3.00 in. (76.2 mm),
- ΔD is the change in borehole diameter in inches,
- ΔQ_h is the change in hydraulic line pressure in psi, and
- T^* is a function of Poisson's ratio and the half contact angle between the jack platen and the rock. [Based on previous studies, we determined Poisson's ratio to be 0.246 and used a T^* value of 1.438 from Heuze and Amadei (1985).]

Values of $\Delta Q_h/\Delta D$ were obtained graphically as the slopes of the linear portion of plots of jack gauge pressure vs the average of the near and far LVDT readings. Figure 4 provides two typical examples of these curves. The linear portion of the loading curve was used in all cases. The low-pressure end of each curve was nonlinear but for most tests the curve became linear at a gauge pressure of 6000 psi (20.7 MPa) or less. As a result, a minimum of three pressure readings was used to establish the linear portion of the curve in all but 1 of 212 post-heat measurements and all but 4 of 64 preheat measurements. Even where boreholes deviated substantially from the ideal diameter D, the curves exhibited linear portions. Half of the tests consisted of two loading and unloading cycles at the same location. These loading cycles commonly showed hysteresis. However, even where hysteresis was quite large, the slopes of the linear portions of the two loading curves were nearly identical.

To correct for longitudinal bending of the jack and thus determine the "true" deformation modulus E_t, one may interpolate in graphs presented by Heuze (1984). These graphical relationships are based on finite element analyses of Heuze and Salem (1976) and experimental results of Meyer and McVey (1974). To expedite calculation of the 64 preheat and 212 post-heat measurements analyzed in this study, we fit an equation to the curve for a rock-mass Poisson's ratio of 0.25, such that

$$E_t = 0.030320 + 0.979484\, E_c - 2.042103 \times 10^{-8} E_c^2 + 1.792758 \times 10^{-13} E_c^3 \quad , \qquad (2)$$

where E_c and E_t are both given in psi.

We considered screening the data according to the full platen seating criterion proposed by Heuze (1984). However, a statistical model of the Heuze screen shows that with high probability, measurements with full platen seating will be rejected and measurements with partial seating will be accepted under conditions that prevail at the SFT—C facility (Axelrod, Patrick, and Yow, 1986). Instead, we have elected to base modulus calculations on the linear portion of the pressure vs displacement curves and to delete modulus values calculated to be greater than 85 GPa. The 85-GPa

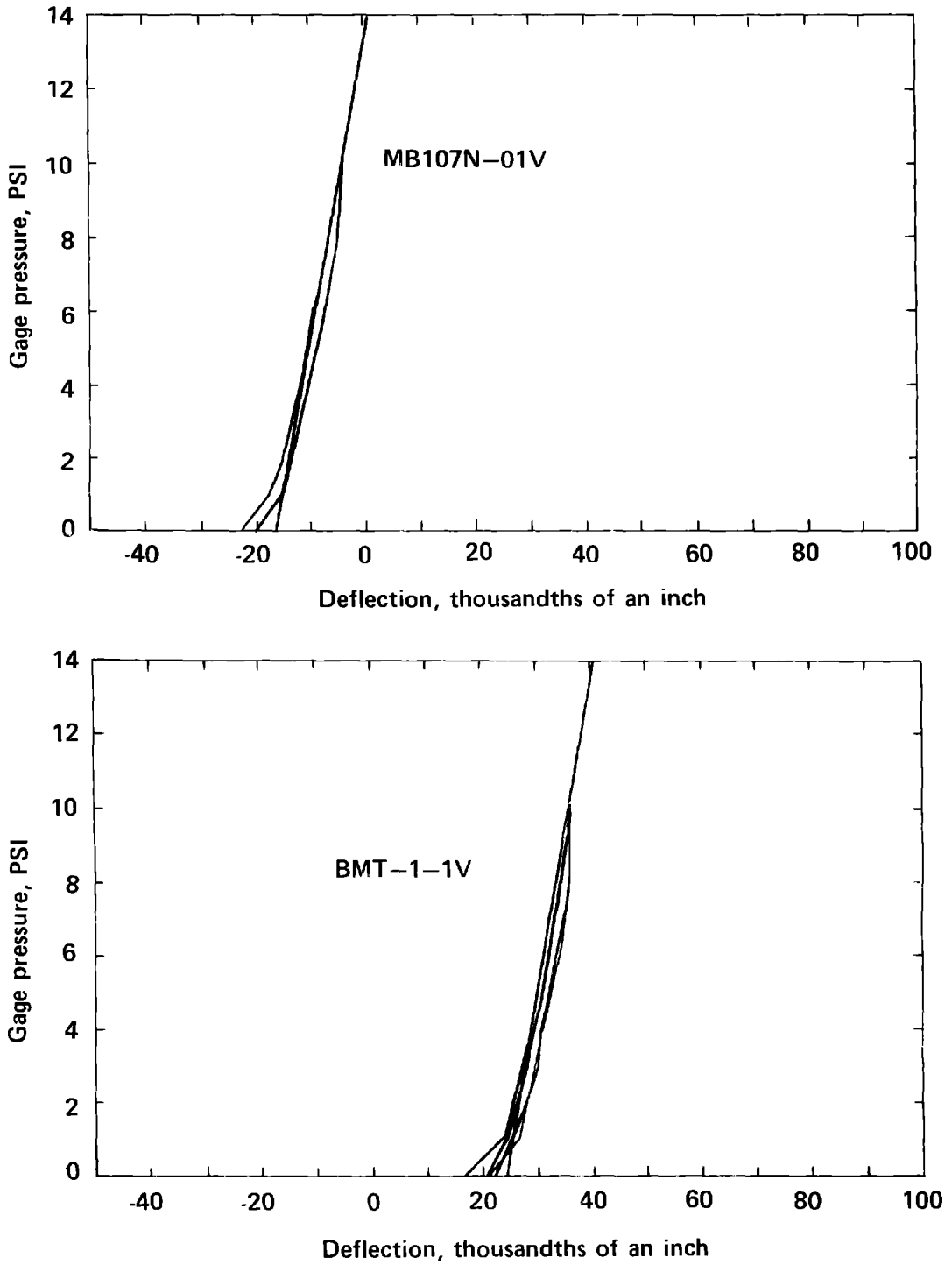

Figure 4. Typical examples of $\Delta Q_h/\Delta D$ plots obtained from undersized (top) and oversized (bottom) boreholes.

cut-off corresponds to the maximum modulus value obtained in biaxial testing of 143-mm-diameter cores. Since the core samples possessed no open fractures, which would reduce the deformation modulus, the laboratory modulus represents an upper bound.

Quantile-quantile plots of the data with the standard normal distribution as a reference (with and without the 85-GPa screening criterion) are shown in Figs. 5a and 5b, respectively. The break in trend of the upper plot lends statistical support to the 85-GPa criterion. The plot in Fig. 5b is linear

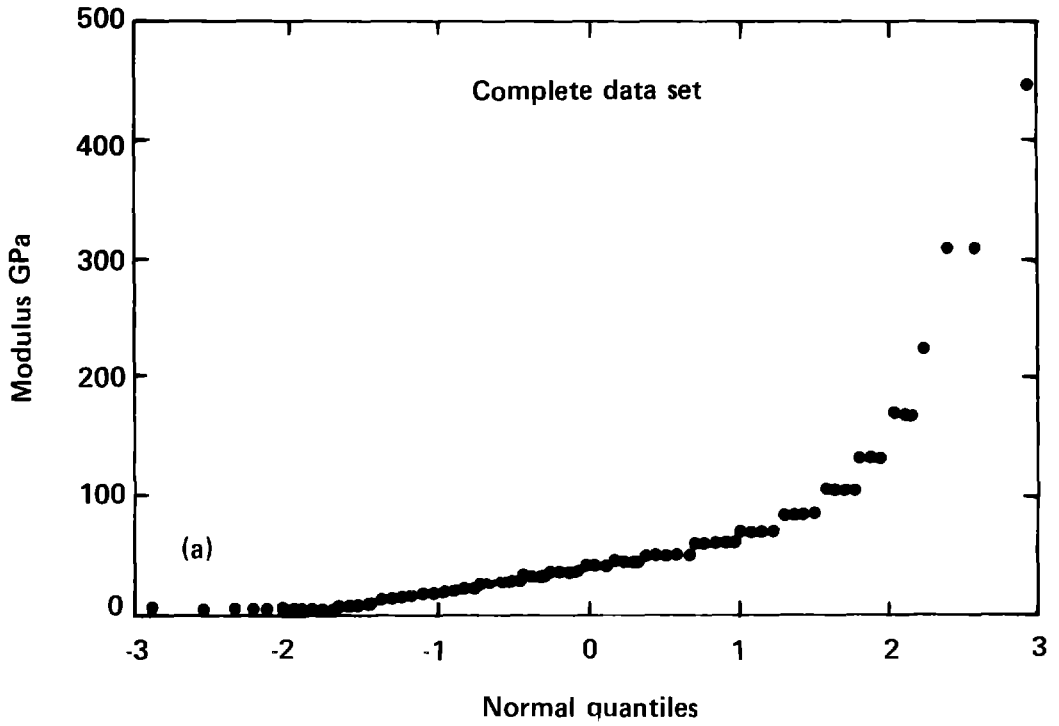

Figure 5a. Plot of ordered values of deformation modulus against normal quantiles for all values of modulus. Horizontal segments are caused by tied values.

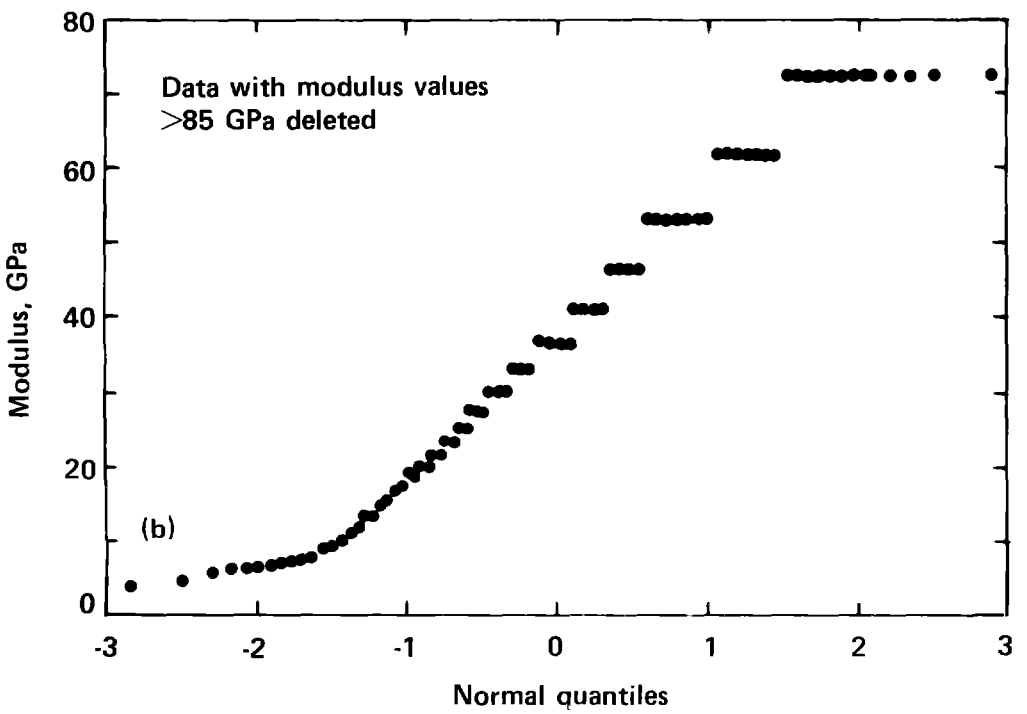

Figure 5b. Plot of ordered values of deformation modulus against normal quantiles for values of modulus less than or equal to 85 GPa. Horizontal segments are caused by tied values.

for modulus values less than 85 GPa except for data below 10 GPa. The trend breaks here because a linear extrapolation of the plot would predict negative modulus values, which are physically impossible.

Only 12 of the 64 preheat data and 17 of the 212 post-heat data are eliminated by this screen, leaving 52 preheat and 195 post-heat data for further analysis. By construction, the screen yields a retention group and a rejection group with different means. Furthermore, even the shapes of the distributions must differ because the screen truncates the upper "tail" of the distribution of modulus values. As noted above, Fig. 5a indicates that 85 GPa is a reasonable value at which to truncate; the higher values seem to come from a different population of measurements. Figure 6 is a rough estimate of the probability density distribution of the complete modulus data set. We see that values greater than 100 GPa are clearly part of a long tail of outliers. Although this plot should only be used for qualitative judgments, it supports the decision to truncate at 85 GPa.

All but three of the 17 measurements deleted by the cut-off screen are from the MBI-series boreholes. The LVDT readings indicate that the boreholes were about 0.468 mm (0.018 in.) undersized at the test locations, about average for this borehole series (Fig. 3). Although some of the pressure vs displacement plots are nonlinear at low pressures, the effect did not appear to be more severe than for measurements that were not deleted. Furthermore, the raw data records show that differences between LVDT readings were generally within 0.100 mm (0.004 in.). Based on these examinations, there is no obvious problem in testing that could explain the anomalously high $\Delta Q_h/\Delta D$ slopes that produced the high modulus values.

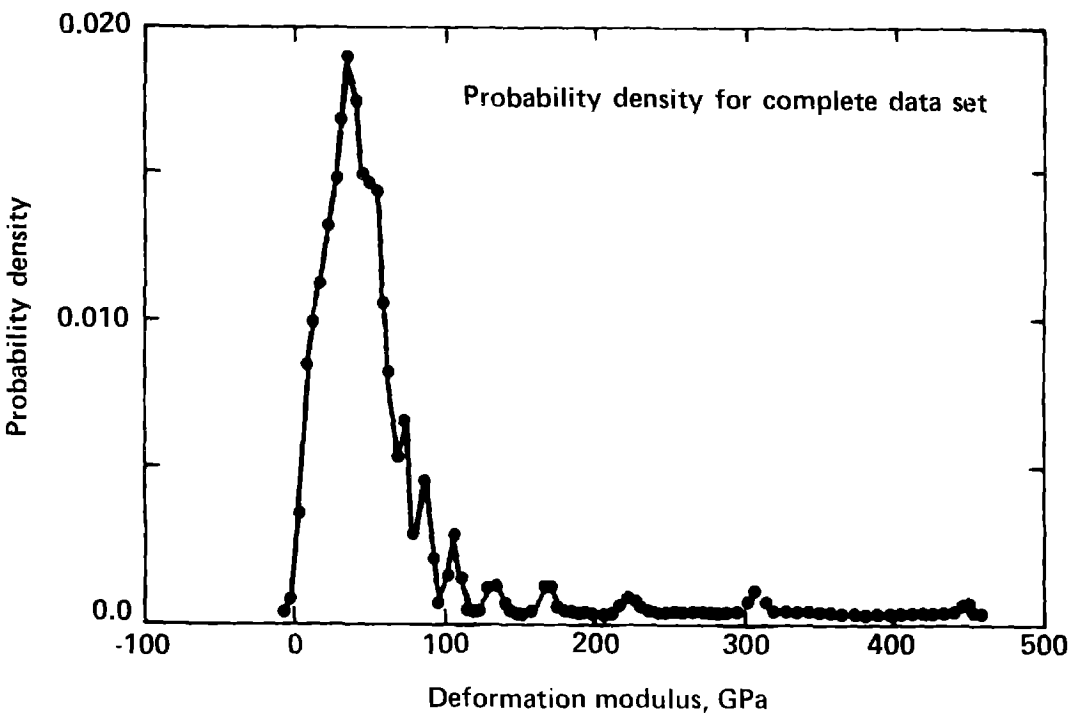

Figure 6. Estimated probability density function of complete deformation modulus data set. The small negative point is an artifact of the calculation. The screen truncates the "tail," i.e., values above 85 GPa.

Results and Discussion

We analyzed the data initially to provide moduli estimates for use in numerical models of rock-mass behavior. The data were then examined to obtain the best possible understanding. First, we simply summarized the data, ignoring spacial dependence and complex interactions among the many variables that may influence modulus values. These summary statistics may be readily used in structural analyses. Second, we thoroughly analyzed aspects of variability in the data set in an effort to better understand how various factors affect rock-mass modulus.

The statistical and graphical techniques applied to the data throughout this report are described in Chambers et al. (1983), Conover (1980), McGill et al. (1978), Searle (1971), and Bradley (1968). The statistical software package "S," developed by Bell Laboratories, was used for many of the analyses [Becker and Chambers (1984)].

Data Summary

The mean modulus before the heating phase of the SFT—C is 30.3 GPa and increases to 39.9 GPa after heating. A rough measure of the accuracy of a mean is the "standard error of the mean" ($\bar{\sigma}$) obtained by dividing the standard deviation of the data by the square root of the number of points used to calculate the mean. There are 52 preheat and 195 post-heat measurements, giving standard errors of 2.41 and 1.27 GPa, respectively. We do not assign any probability interpretations (such as confidence intervals) to these standard errors since a more detailed and accurate analysis will be done later. Table 5 summarizes pertinent statistics for each loading direction and level of heating. The "no heat" data were obtained from the four pillar boreholes before heating, and the "moderate heat" data were obtained from the same four boreholes plus UG02 following the 3-year heated phase of the SFT—C. Throughout this report, data from these two time periods are referred to as preheat and post-heat, respectively. The data receiving the "high heat" treatment came from boreholes NHH10A and SHH05A, which are located near electrical heaters.

The highly variable nature of the modulus data is clearly evident in the "box plot" for each borehole shown in Fig. 7. This presentation conveys several important items of information. For each box, a measure of the range of the data is displayed by the vertical line segment that extends to 1.5 times the inner quartile value. When extreme data values occur, they are plotted as individual points above or below this vertical segment. The median is indicated by a horizontal line segment in the middle of a tapered notch, which can provide a rough measure of the statistical significance of the difference between two medians. If the notch of one box falls outside the notch of another box, the medians of the two data sets are different at approximately the 5% level (McGill et al., 1978). Since the height of the box is established by the interquartile range* of the data, it is a measure of the variability of the data. The box

* For Gaussian data, the interquartile range = 1.349 σ, where σ is the theoretical standard deviation of the data.

Table 5. Comparison of effects of heating and loading direction on deformation modulus.

Direction	Treatment: No heat (18–24°C)[a]	Moderate heat (30–40°C)[a]	High heat (55–65°C)
Vertical loading	E = 31.2[b]	42.2	—
	n = 26 σ = 3.47	42 2.76	
N61°W loading	29.5	35.8	24.7
	26 3.41	43 2.61	17 3.81
N29°E loading	—	51.6	22.6
		11 4.55	17 2.84

[a] Data from pillars only.

[b] E = mean deformation modulus, GPa, n = number of data.
$\sigma = S/\sqrt{n}$ = standard error of the mean, GPa, where
S = sample standard deviation, GPa.

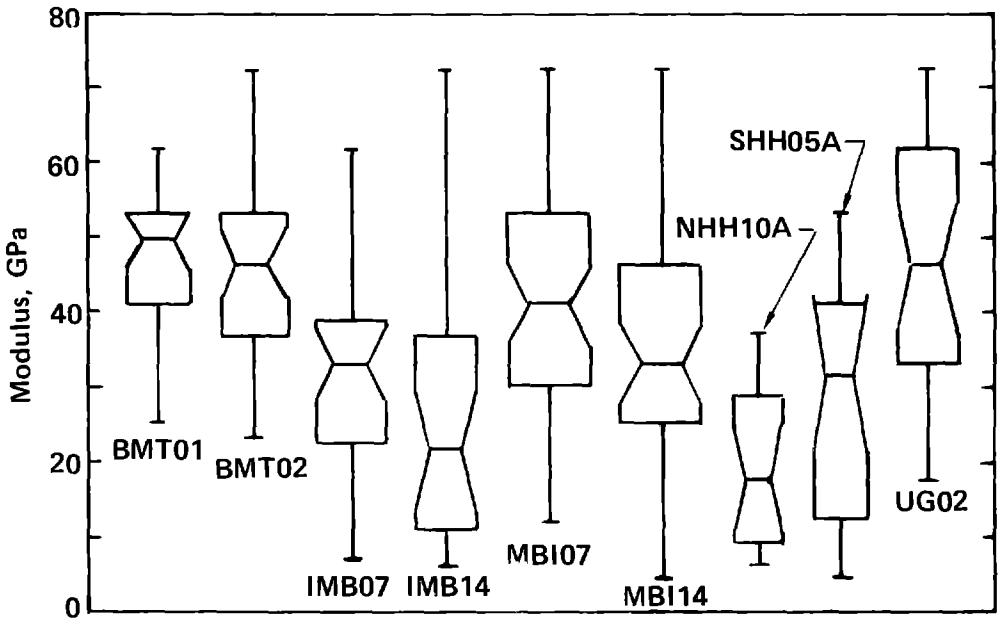

Figure 7. Box plots of pre- and post-test deformation modulus data grouped by borehole. Modulus values greater than 85 GPa have been screened from the data set. Note: The median value occurs at the notch, the box height is the interquartile range, the vertical line segment spans 1.5 times the interquartile range, and the box width is in proportion to the $\sqrt{n}$.

width is in proportion to the square root of the number of data in the group represented by the box. This is a natural scaling because the accuracy of the mean scales by $1/\sqrt{n}$.

The data as summarized in Table 5 and Fig. 7 are spacially variable on at least an inter-borehole scale. Moreover, the modulus is anisotropic and heat-sensitive. This suggests a need for further analysis of the magnitude and statistical significance of these factors.

Statistical Analysis of Data

Our basic approach in analyzing the 247 values obtained from pre- and post-heat measurements is to develop linear models composed of individual factors and interactions among these factors. By its very nature, model building is usually a trial-and-error endeavor and our case is no exception. Based on physical principles and empirical knowledge, an initial model is developed that incorporates the factors that are thought to be significant. These factors are then tested for significance and deleted if appropriate. Until a satisfactory model is obtained, new factors are added and tested sequentially. In examining the quality of the models developed here, it is important to realize the magnitude of the error contributed by the measurement technique. An analysis of measurement errors (presented in Appendix C) shows that we can expect a variability (1σ) of about ± 6 GPa from the measuring system alone. This error should be compared with the residual standard errors, which range from 9.5 to 13.5 GPa for the models used in this study. Models for single boreholes and groups of similar boreholes are discussed in turn below.

Pillar Boreholes

As shown in Fig. 2, four boreholes are located in the two pillars that were created as a result of constructing the SFT—C. These boreholes, which are designated MBI07N, MBI07S, MBI14N, and MBI14S, were drilled during construction of the facility so both pre- and post-heat deformation modulus measurements were obtained in them. Because of the close proximity of the boreholes and the similarity of excavation techniques used in the drifts, we chose to evaluate the data from these four boreholes using as few models as possible. This approach allowed us to make rather straightforward assessments of the effects of various factors on the deformability.

Our preliminary examinations of the data revealed that the within-hole spacial variability of the post-heat data from MBI14N was fundamentally different from that of the other pillar

boreholes. Whereas the data from the latter three borehole segments indicated that modulus values were greatest near the pillar center and decreased toward the drifts, the opposite occurred in MBI14N. As a result, it was necessary to develop a separate model for MBI14N. We elected to include both pre- and post-heat data in this model so that the effects of heating could be evaluated.

In examining the data from boreholes MBI07N, MBI07S, and MBI14S, we found the following four factors to be influential: position within the borehole, location within the facility, loading direction, and heat. The appropriate variable to describe the position within the borehole is the distance of the measurement from the center of the borehole, a quantitative variable. Distance from borehole center was selected as the variable because rock damage caused by blasting and by stress changes should be present at each outer surface of the pillars, lending symmetry to the effect. The other factors are all qualitative, so an analysis-of-covariance model is convenient (Searle, 1971).* Each of the qualitative factors has only two levels: north or south pillar, vertical or horizontal loading, and pre- or post-heat, respectively. In addition to the influence of individual factors, significant interactions between heat and loading direction and between heat and pillar location were detected.

The three factors at two levels require six terms, the two sets of interactions require four additional terms, and the constant and slope coefficient add two more, for a total of 12 terms. Since no "station" effect (that is, 07 vs 14) was detected and a common slope applies, one model was developed for all three boreholes. The resulting linear statistical model applies to the data from MBI07N, MBI07S, and MBI14S. Expressed for the ith data value, where i = 1 to 104,

$$E_i = \mu + \beta d_i + \sum_{j=1}^{10} X_{ij}\,\gamma_j + \epsilon_i \quad , \tag{3}$$

where E_i = deformation modulus (GPa), d_i = distance of the measurement from the borehole center, and the X_{ij} are factor variables. When the jth factor is present, $X_{ij} = 1$; when absent, $X_{ij} = 0$. The model parameters are μ, β, and γ_j, and the ϵ_i represent residual errors. It is important to note that the ϵ_i contain all known and unknown sources of error. If the model explained all sources of variation, the ϵ_i would represent only random measurement error. As noted previously, an error of about ± 6 GPa (at 1σ) would remain because of inaccuracies in the measuring system (Appendix C).

Although the parameterization of the model is not unique, all parameterizations will give the same results. The model parameters cannot be estimated separately, as is the case for regression. Instead, only certain meaningful linear combinations are estimated using the singular-value decomposition technique. Of a total of 123 measurements, 19 were discarded because they exceeded the 85-GPa limit of the data screen. Using the model given by Eq. (3), we analyzed the remaining 41 preheat and 63 post-heat modulus values from the three borehole segments.

Table 6 lists the "intercept" terms for the various data subsets that were analyzed. These intercepts represent the mean modulus values at the pillar center. The overall slope of the 104 data is -7.0 GPa/m. This global model explains about 44% of the variability in the data, and the residual error for the data using this model is about 13.5 GPa (Table 7). There is a price associated with using a model such as this. Because the fit applies to three boreholes under all conditions, it does not fit some individual cases as well as a model restricted to apply only to that case; for an example, see Fig. 8.

The physical interpretation of these coefficients is straightforward. For example, the predicted value of the post-heating modulus under

* If all the variables were quantitative, we would use regression analysis.

Table 6. Intercept coefficients calculated using a 12-term linear model for deformation modulus (GPa). Data from boreholes MBI07N, MBI07S, and MBI14S.

Time of measurement	North pillar (GPa)		South pillar (GPa)	
	Vertical loading	Horizontal loading	Vertical loading	Horizontal loading
Preheating	46.5	57.2	26.3	37.0
Post-heating	62.7	52.9	54.6	44.8

Table 7. Summary statistics for the covariance model of deformability (boreholes MBI07N, MBI07S, MBI14S).

Residual standard error (GPa)	R^2	North pillar (GPa)				South pillar (GPa)				Slope (GPa/m)	t value slope	n
		Preheat		Post-heat		Preheat		Post-heat				
		Vert.	Horiz.	Vert.	Horiz.	Vert.	Horiz.	Vert.	Horiz.			
13.53	0.44	46.54	57.23	62.71	52.87	26.26	36.96	54.63	44.80	−6.96	4.26	104

horizontal loading in the north pillar is 52.9 GPa at the pillar center, and it decreases 7.0 GPa/m from the center in either direction. The data from each borehole and associated regression lines from the covariance model are shown in Figs. 8–13.

Since this model uses a common slope, it is relatively easy to interpret the effect of the various factors. First, there is a strong anisotropy in the modulus. Before heating, the rock mass modulus is about 10.7 GPa less in the vertical loading direction in both the north and south pillars, indicating that the more frequent low-angle joints (which are infilled with pyrite, sericite, and quartz) tend to affect the modulus more than the high-angle joints (which appear "open" at free surfaces but are typically clean or infilled with calcite). Second, while the anisotropy remains after the episode of heating, the modulus is now about 9.8 GPa greater in the vertical loading direction. This is consistent with a hypothesis that the stresses increase as a result of thermal expansion of the rock, thereby increasing joint stiffness. Thermomechanical calculations indicate that the vertical stresses at the time of the post-heat measurements were about 5 MPa (40%) greater and horizontal stresses were as much as 2 MPa (20%) less in the pillar center than they were before the episode of heating (Butkovich, 1981). Third, note in this context

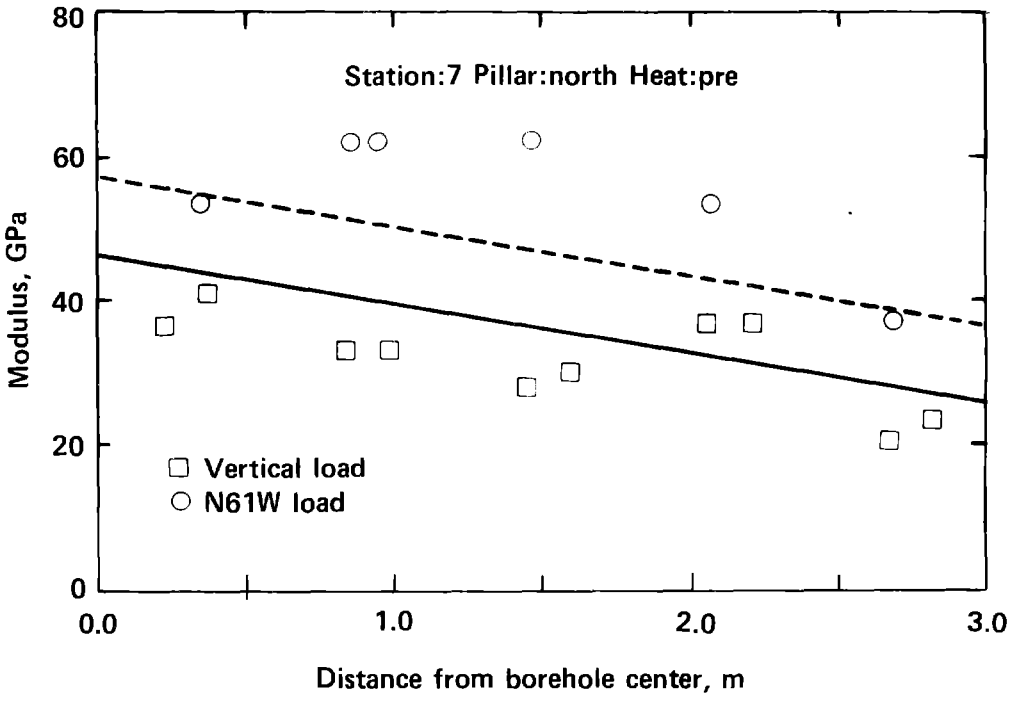

Figure 8. Relationship between borehole modulus value and distance from pillar center for pretest data from MBI07N. The slope and intercepts of the lines were developed from a 12-term linear model.

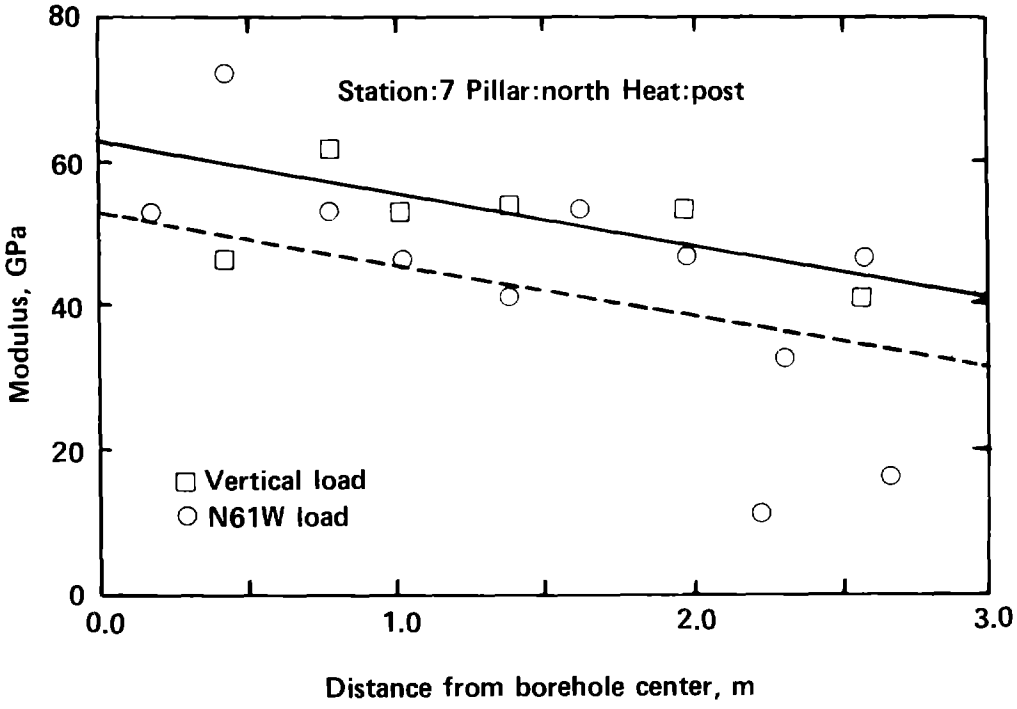

Figure 9. Relationship between borehole modulus value and distance from pillar center for post-test data from MBI07N. The slope and intercepts of the lines were developed from a 12-term linear model.

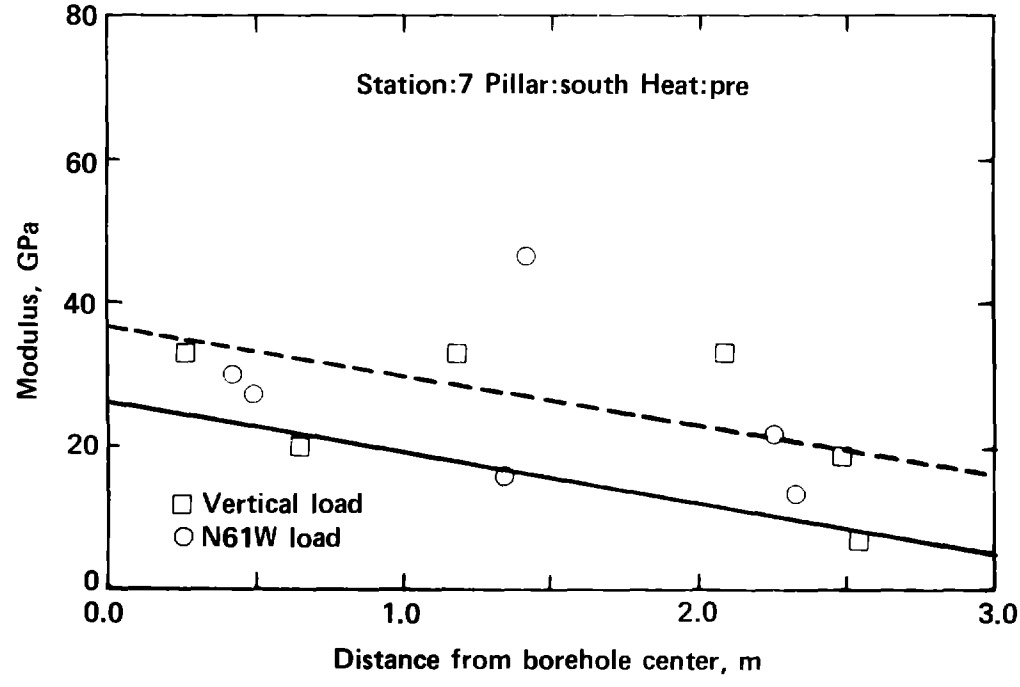

Figure 10. Relationship between borehole modulus value and distance from pillar center for pretest data from MBI07S. The slope and intercepts of the lines were developed from a 12-term linear model.

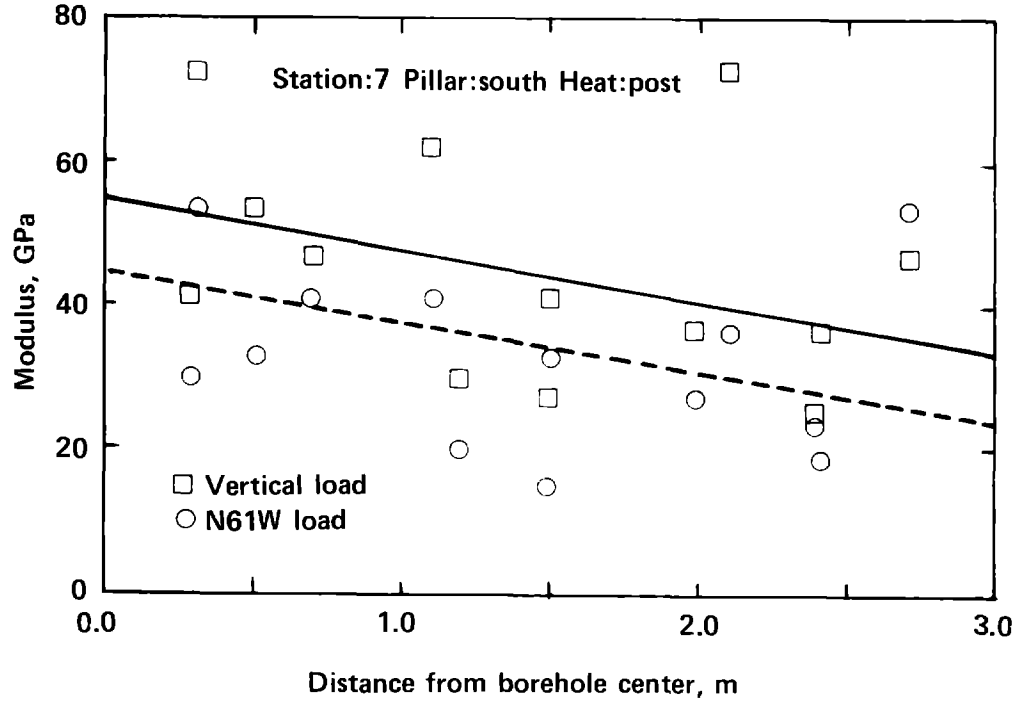

Figure 11. Relationship between borehole modulus value and distance from pillar center for post-test data from MBI07S. The slope and intercepts of the lines were developed from a 12-term linear model.

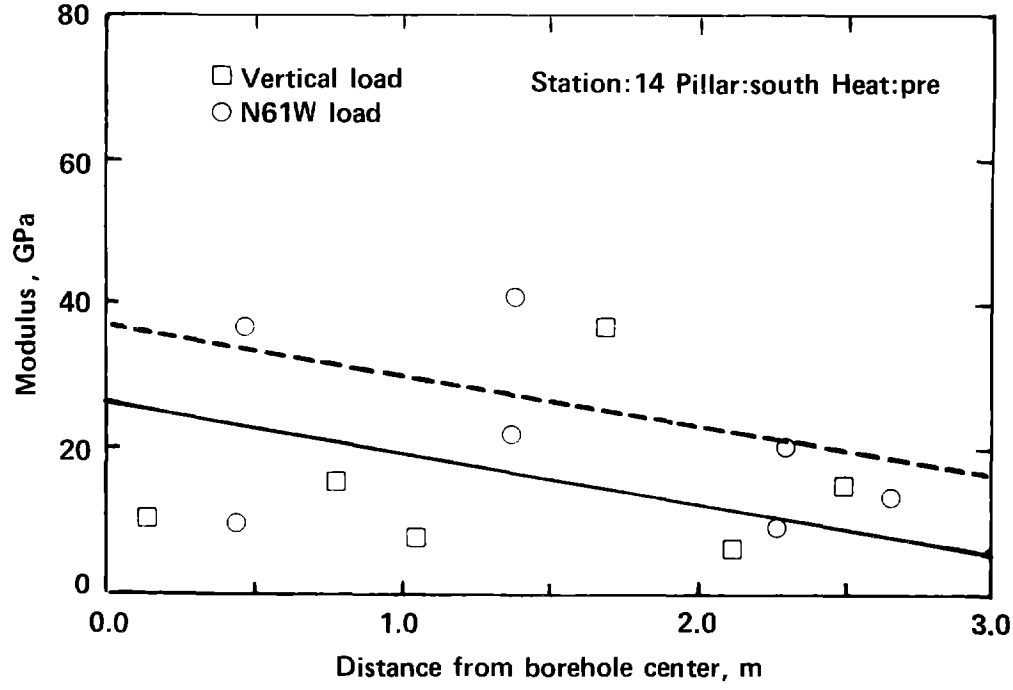

Figure 12. Relationship between borehole modulus value and distance from pillar center for post-test data from MBI14S. The slope and intercepts of the lines were developed from a 12-term linear model.

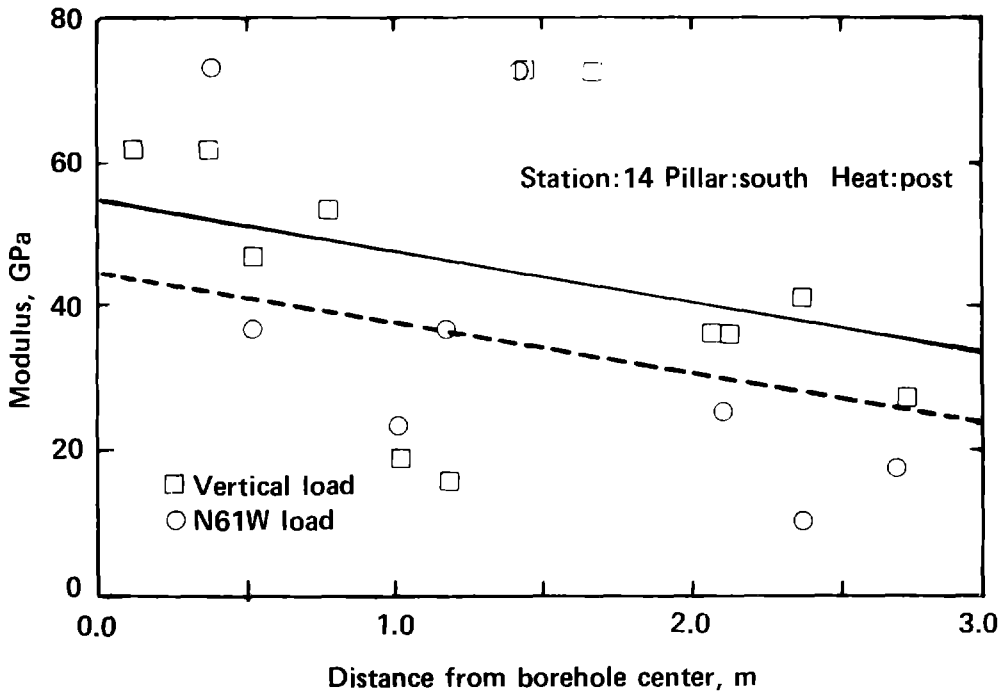

Figure 13. Relationship between borehole modulus value and distance from pillar center for post-test data from MBI14S. The slope and intercepts of the lines were developed from a 12-term linear model.

that the modulus for vertical loading increased by 16.2 to 28.3 GPa, whereas the modulus for horizontal loading in one case decreased by 4.3 GPa and in the other increased by only 7.8 GPa. This is compatible, in concept, with our understanding of the influence of stress changes on individual joints (Goodman, 1980, and Yow, 1985). Nearly all test pressure-vs-deformation curves exhibited linear behavior above a given level of loading. With a maximum load applied to the rock of about 0.703 MN (158,000 lb) on opposing 0.2-m-long (8-in.) platens, this linearity appears to be in agreement with the linearity obtained in normal loading of individual joints by Bandis et al. (1983).

Data from the fourth pillar borehole were analyzed separately because of obvious differences in the spacial character of the data. Seven of the 40 measurements were discarded by the 85-GPa cut-off screen. In addition, an eighth measurement (72 GPa) was discarded when it was judged to be a statistical outlier.

Examination of the preheat modulus values from MBI14N indicates strong anisotropy (Fig. 14). However, a statistical test for zero slope confirms that there is no depth effect for either loading direction. Using a very simple model consisting of a loading direction effect and an intercept, we find that the mean modulus value for vertical loading is about 45 GPa greater than for horizontal (N61°W) loading. As discussed below, this is consistent with the high intensity of vertical fracturing observed in this pillar. In light of a residual standard error of 6.6 GPa, this is highly significant.

Turning to the post-heat modulus values from MBI14N, we see a strong depth effect (Fig. 15). For this analysis, the data were pooled because we could not detect a significant difference between the two loading directions. With the exception of the last four points, matched pairs from the two loading directions differ by less than 5 GPa. (The matched pair analysis is elaborated on in the following discussion of data from the heater drift boreholes.) We found that introducing a second-order depth term improved the fit compared with a single-term model. About 50% of the variation in modulus is explained by a model of the form

$$E_i = \mu + \beta_1 d_i + \beta_2 d_i^2 + \epsilon_i \quad , \qquad (4)$$

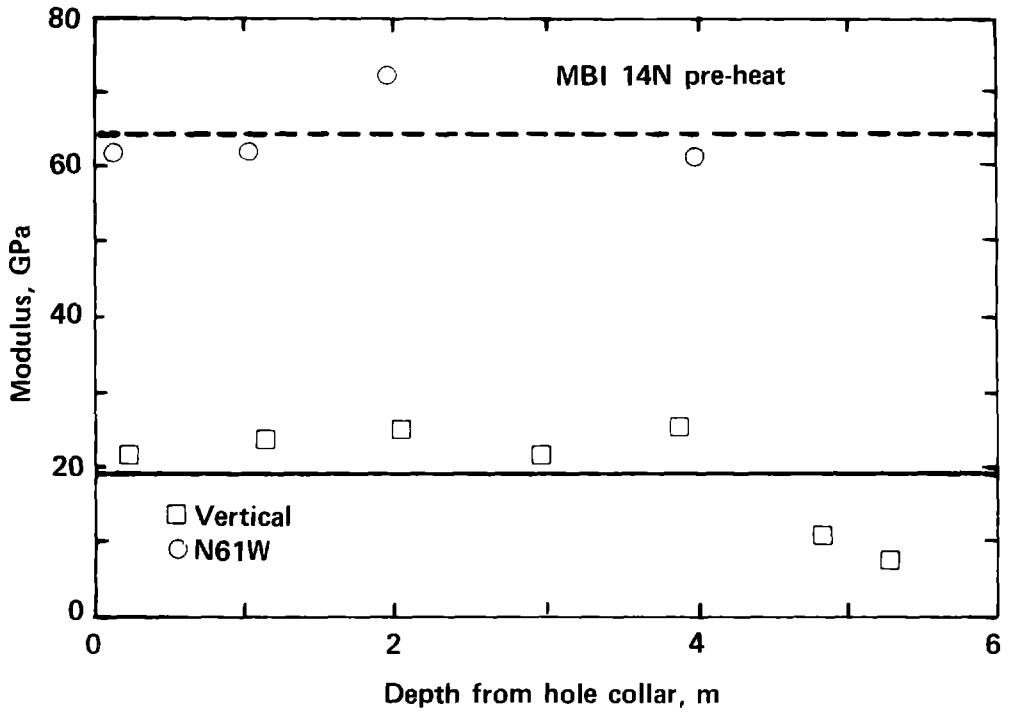

Figure 14. Relationship between borehole modulus value and distance from pillar center for post-test data from MBI14N.

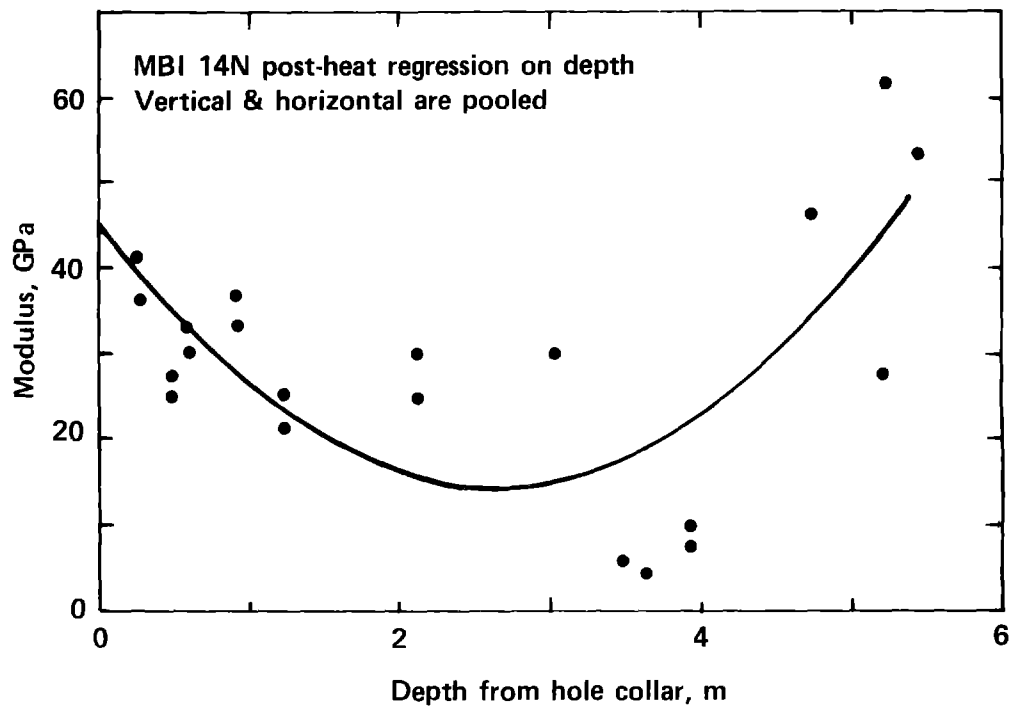

Figure 15. Relationship between borehole modulus value and distance from borehole collar for post-test data from MBI14N.

where d_i is distance from borehole collar and the remaining terms are as previously defined. A least-square fit of Eq. (4) to the data gives parameter values of $\hat{\mu} = 44.9$, $\hat{\beta}_1 = -23.2$, and $\hat{\beta}_2 = 4.41$ (Table 9). Using these values, we calculate a modulus value at pillar center of 14.4 ± 4.4 GPa. The residual standard error of 11.2 GPa is consistent with that of the other data sets (Tables 7, 8, and 9).

Because the models for preheat and post-heat modulus values are so fundamentally different, determination of the effects of heating is not as simple as it was for the data from the other three pillar boreholes. Table 10 would seem to indicate simply that heating dramatically decreased the modulus for vertical loading and slightly decreased it for horizontal loading. While this is true at the pillar center, Figs. 14 and 15 indicate that near the outer surfaces (ribs) of the pillar the modulus for vertical loading decreased very little and the modulus for horizontal loading increased significantly.

A possible explanation for these unusual depth and heating effects on modulus is found in the character of the geologic fracturing observed in the vicinity of borehole MBI14N. The degree of fracturing near the pillar center (as observed in the borehole and projected from tunnel mapping) is much more intense than for other boreholes (Wilder and Yow, 1981 and 1984). Since these fractures are near vertical and are oblique to the borehole axis, they would tend to decrease the modulus under horizontal loading. As noted earlier, modulus values are expected to increase with increasing stress. Our observation that modulus values increased near the ribs and remained unchanged or decreased near the pillar center could suggest that similar changes occurred in the pillar stresses. We did not acquire enough stress data to directly address this possibility, but the continuum calculations (which ignore the presence of fractures) suggest that the opposite occurred.

Heater Drift Boreholes

At the completion of the SFT—C, an opportunity was available to obtain deformability measurements in two boreholes located near electrical heaters. Boreholes NHH10A and SHH05A were drilled where rock temperatures were about 60°C for a 3-year period. Because these boreholes were unavailable for testing at ambient temperature, only post-heating data can be analyzed.

Plots of deformation modulus vs depth from hole collar are shown for NHH10A in Fig. 16 and

Table 8. Regression summary for straight line models of deformability.

Borehole	Residual standard error (GPa)	R^2	F	Intercept (GPa)	Slope (GPa/m)	t value Intercept	t value Slope	n	Comment
NHH10A	9.59	0.18	2.99	11.68	6.91	2.45	1.73	16	Pooled loading, distance from center
SHH05A	9.53	0.62	26.61	49.98	- 8.30	10.36	-5.16	18	Pooled loading, depth from hole collar
UG02	10.01	0.71	43.48	76.26	- 7.83	16.00	-6.59	20	3 end points deleted, pooled, distance from center
BMT02	10.02	0.05	0.71	46.68	-0.45[a]	11.20	-0.84	14	Pooled loading, depth from hole collar, no spacial effect

[a] Not significant, true slope may be zero.

Table 9. Regression summary for the square law models of deformability.

Borehole	Residual standard error (GPa)	R^2	F	Intercept (GPa)	β_1 (GPa/m)	β_2 (GPa/m^2)	t value Intercept	t value β_1	t value β_2	n	Comment
BMT01	11.05	0.19	2.68	40.92	3.79	- 0.27	7.36	1.98	- 2.21	26	Pooled, distance from hole collar
MBI14N	11.18	0.48	8.34	44.91	- 23.23	4.41	7.65	3.85	4.06	21	Pooled, post-heat, distance from hole collar

Table 10. Comparison of deformation modulus values (GPa) at the center of the pillar. Data from MBI14N.

Time of measurement	Vertical loading	Horizontal loading
Preheat	64.3	19.2
Post-heat	14.4	14.4

SHH05A in Fig. 17; the loading directions have been coded by the indicated symbol. A systematic variation of modulus with depth is evident in both holes and for both loading directions. The very low values of modulus in borehole NHH10A are closely associated with a highly fractured zone where the Receiving Room fault intersects the borehole at a depth of about 2 m (Wilder et al., 1982). Likewise, the observed trend in SHH05A coincides with the profile of increasing temperature (Fig. 18).

The presence of spacial correlation in the measurements complicates the analysis, as it did in the MBI boreholes. However, the plots suggest that the depth effect is the same for both loading directions, so a model may be developed of the form

$$E(i,k) = f[d(i)] + \epsilon(i,k) \quad ; i = 1,2,3,\ldots n \quad , \qquad (5)$$

where

- $E(i,k)$ = deformation modulus in the borehole in loading direction k,
- $d(i)$ = depth from hole collar,
- $\epsilon(i,k)$ = random disturbance term,
- k = 1 for N29°E loading direction,
- k = 2 for N61°W loading direction,
- n = number of measurements in borehole under consideration.

To examine the loading direction effect, we form the quantity $\delta(i)$ given by

$$\delta(i) = E(i,1) - E(i,2) = \epsilon(i,1) - \epsilon(i,2) \quad . \qquad (6)$$

If $\epsilon(i,1) = \epsilon(i,2)$, there is no loading direction effect.

For the analysis based on Eq. (6) to be valid, the $\delta(i)$ must be independent of depth. Note that we are testing whether the *differences* in modulus values are correlated with depth, not whether the *values* are correlated with depth. For boreholes NHH10A and SHH05A, the values of Kendall's test statistic S are 4 and −2, which are not significant (Bradley, 1968). Thus, we have shown that

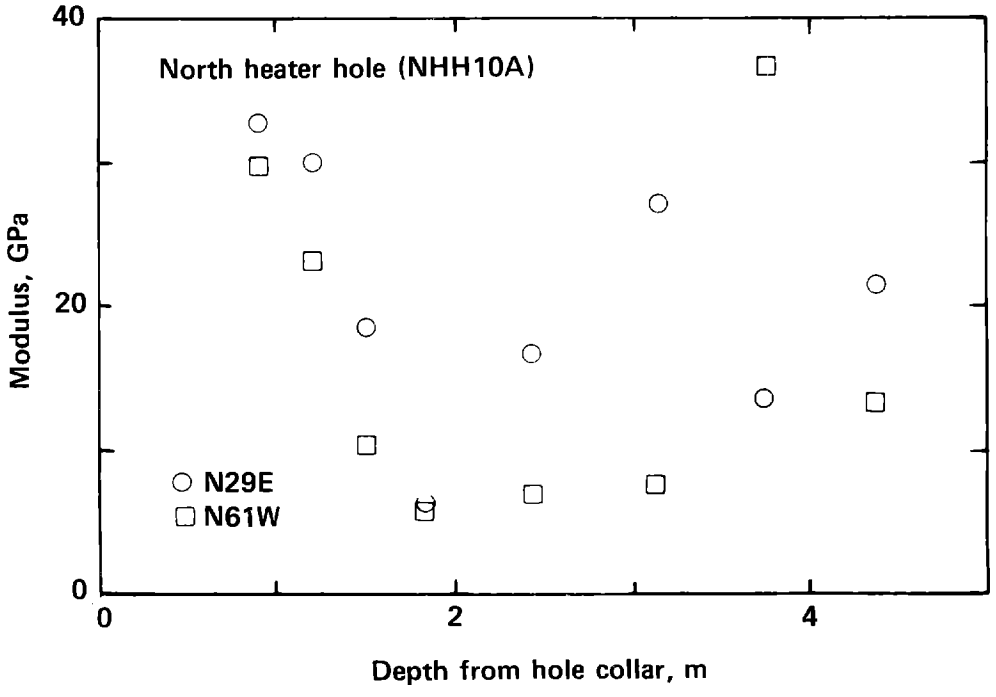

Figure 16. Relationship between borehole modulus value and distance from borehole collar for borehole NHH10A.

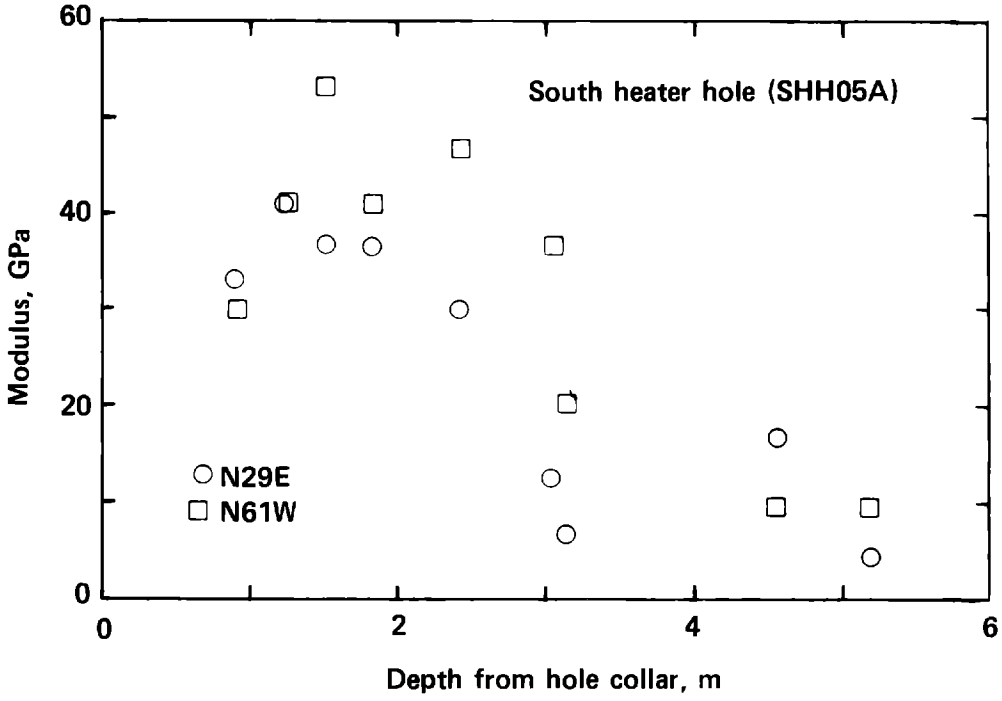

Figure 17. Relationship between borehole modulus value and distance from borehole collar for borehole SHH05A.

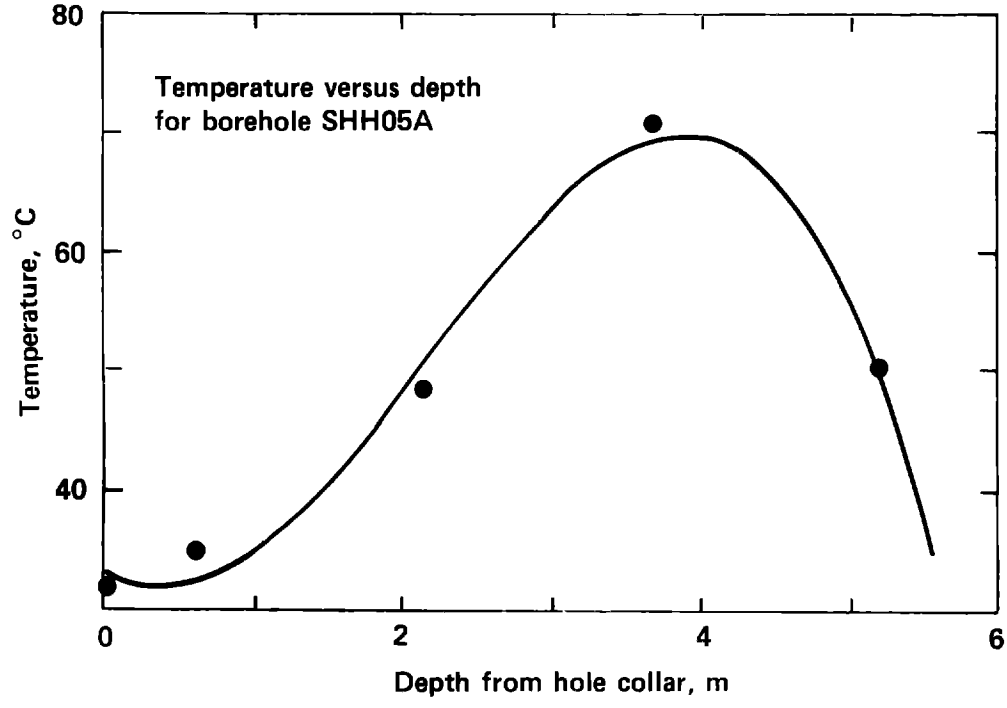

Figure 18. Temperature profile at the location of borehole SHH05A.

the depth effect is the same for both loading directions in the heater holes (or is too small to be detected with this sample size). The same $\delta(i)$ can be used to determine if a loading direction effect is present. Since we have so few data (only eight paired measurements in the north heater hole and nine in the south), the nonparametric sign test can be used to test the hypothesis that the median values for the two loading directions are equal.

For NHH10A, seven of the eight deltas are positive, giving a two-sided significance level of $p = 0.07$.* Although we consider this to be marginal evidence for anisotropy, the indication is that modulus values obtained under N29°E loading are slightly greater than those obtained under N61°W loading.

Conversely, the SHH05A hole has six negative, two positive, and one zero delta. The presence of the zero value complicates the application of the sign test. However, whether we ignore the point or count it as positive or negative, we fail to detect a statistically significant difference with the sign test. Moreover, the N61°W loading modulus tends to be greater than the N29°E modulus, the reverse of the north heater hole. If we regard the two heater holes to be similar, then the marginal $p = 0.07$ for NHH10A appears even weaker: the two data sets taken together would suggest no detectable loading direction effect. However, if we regard the two heater holes as different experiments, then the sign test yields opposite inferences: marginal significance ($p = 0.07$) for NHH10A and no significance for SHH05A. Since there are so few measurements, our conclusions concerning anisotropy in these boreholes remain equivocal.

If we proceed to pool the data from the two loading directions, we can fit linear models of modulus as a function of depth for each borehole. Higher order functions did not produce commensurate improvements in the fit. For NHH10A, we take advantage of symmetry about the rubble zone at 2 to 2.4 m depth and index the depth from borehole center. The resulting regression is quite poor by some standards: it explains less than 20% of the variability in the data. However, the residual error of 9.6 GPa is consistent with that of the other models (Tables 7, 8, and 9). Coefficients of $\hat{\mu} = 11.7$ GPa and $\hat{\beta}_1 = 6.9$ GPa/m are determined by the linear model (Table 8 and Fig. 19). This slope term provides a measure of the combined effects of the nearby fault and long-term heating of the rock. It is similar in magnitude but opposite in sign from the slope term for the MBI-series boreholes. The relatively poor fit to the data is the result of fracture-related variability in the data. Presumably, if we knew the relationship between fracture characteristics (both the properties and orientations) and measurement of the modulus, we could explain much more of this variability with a model.

A regression of modulus on depth from borehole collar for SHH05A explains about 62% of the variability in the data and provides coefficients of $\hat{\mu} = 50.0$ GPa and $\hat{\beta}_1 = -8.3$ GPa/m (Fig. 20). The residual error of 9.5 GPa is consistent with that of other models (Tables 7, 8, and 9).

The observed decrease in modulus with depth mirrors the increase in temperature with depth that was caused by the nearby heaters (Fig. 18), suggesting a heating effect on modulus. In the absence of preheating data from this borehole, it is not possible to conclusively establish that a heating effect is present. However, such an effect is plausible. Thermomechanical calculations suggest that the rock stresses increased by about 5 MPa from initial values of 5.5 to 12.5 MPa as a result of heating and associated thermal expansion (Butkovich, 1981). Conceptually, the clays that are commonly present as joint infillings could have been "overconsolidated," and calcite asperities could have been crushed by the thermal stresses. After the rock mass cooled, the joint infillings would not completely recover their initial volume so that at stresses below the overconsolidation stress, the walls of the joints and the clay would form a more compliant system than existed before the heating cycle. Although more pronounced in these boreholes, this effect is consistent with the observation in the MBI boreholes of slight increases or decreases in modulus under horizontal loading (rather than the pronounced increases observed in most cases for vertical loading).

An effect of this type has been observed in tests by Bandis et al. (1983) where normal stresses were cycled from zero to 30–50 MPa. However, this comparison can be made in only a qualitative way at this time since Bandis et al. did not publish results from cycles of loading that were lower in magnitude. The threshold loading above which damage to discontinuity asperities occurs is thus undefined.

Other explanations of the observed decreases in modulus have also been considered but rejected. Laboratory studies of microfracture density

* Which value of p is "significant" is an arbitrary judgment—$p = 0.05$ is widely used, but the selection of a p value should be based on the "cost" of making a wrong conclusion.

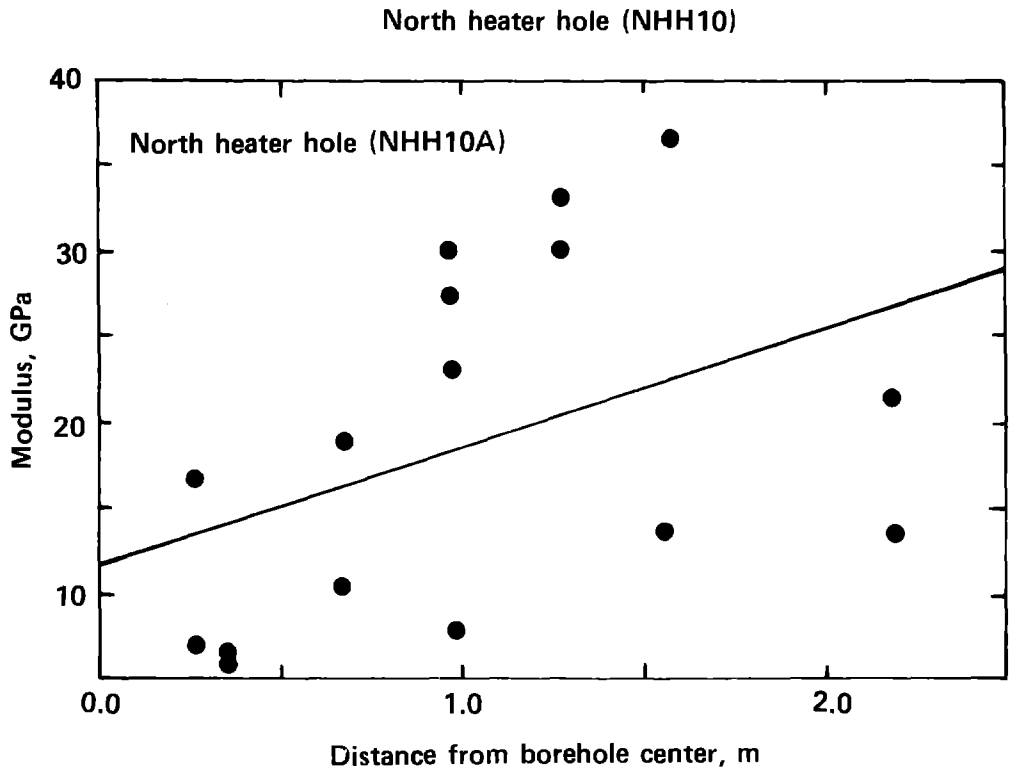

Figure 19. Relationship between modulus value and distance from borehole center for NHH10A. Data are pooled and the linear regression is superimposed on the data.

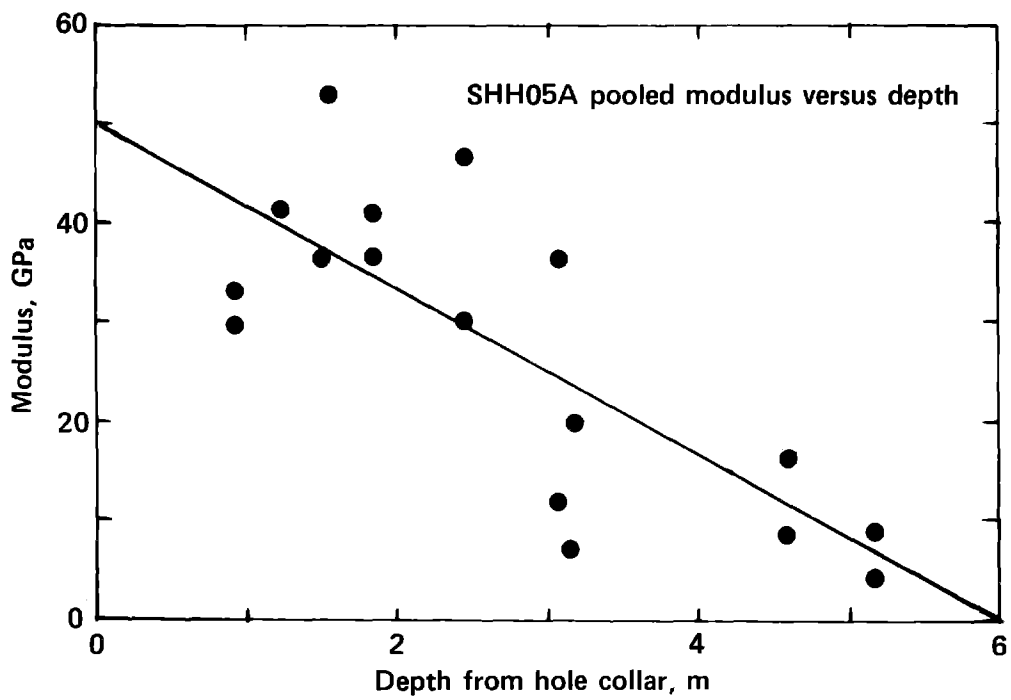

Figure 20. Relationship between modulus value and distance from borehole collar for SHH05A. Data are pooled and the linear regression is superimposed on the data.

in stressed and irradiated Climax quartz monzonite show very little additional microfracture development, even at stresses close to failure (Beiriger and Durham, 1984). Likewise, work by Ryerson and Qualheim (1983) suggests little likelihood of mineral dissolution at the temperature and moisture conditions present near the heater boreholes.

Abutment Boreholes

The two boreholes designated BMT01 and BMT02 were drilled outward from the SFT—C to examine the distribution of deformation modulus values in the abutments of the facility (Fig. 2).

Since there is a pair of orthogonal measurements at each depth for BMT01, we apply a "matched pair" technique. Because spacial correlations are so prevalent in data of this type, Kendall's test (Bradley, 1968) is used to evaluate the possibility that the loading-direction effect is, itself, a function of depth. Kendall's test failed to detect any correlation between loading direction and depth, when depth was measured from borehole collar or from borehole center. Having established that there is no spacial effect on loading direction, the sign test was applied to test the hypothesis that the median difference in modulus values for the two loading directions was zero. Seven of the differences are positive, three are negative, and three are zero. If we assume that the zero values are solely the result of lack of resolution in the measurements, the true signs are unknown. Assigning a positive sign to the zeros would favor rejection of the hypothesis. In this case, there are 10 positive signs and 3 negative signs, giving a significance level of $p = 0.10$. However, if only one of the zeros is really negative, then $p = 0.5$. The sign test thus fails to detect any difference in the medians. If we believe the modulus measurements are normally distributed, then the more sensitive t-test may be used. However, the associated t-value of 1.29 is also not significant. Thus, the parametric and nonparametric analyses are consistent in their conclusions.

Based on the results of these tests, the data from BMT01 for both loading directions may be pooled. By applying a regression model of the form of Eq. (4), we obtain parameter estimates $\hat{\mu} = 40.9$, $\hat{\beta}_1 = 3.79$, and $\hat{\beta}_2 = -0.274$ (Table 9). The data from BMT01 and the associated curve are shown in Fig. 21. The model explains only about 20% of the variability in this data set, and the residual error of 11.0 GPa is consistent with that of the other models (Tables 7, 8, and 9).

Turning to borehole BMT02, we see no obvious depth or loading direction effects in a plot of

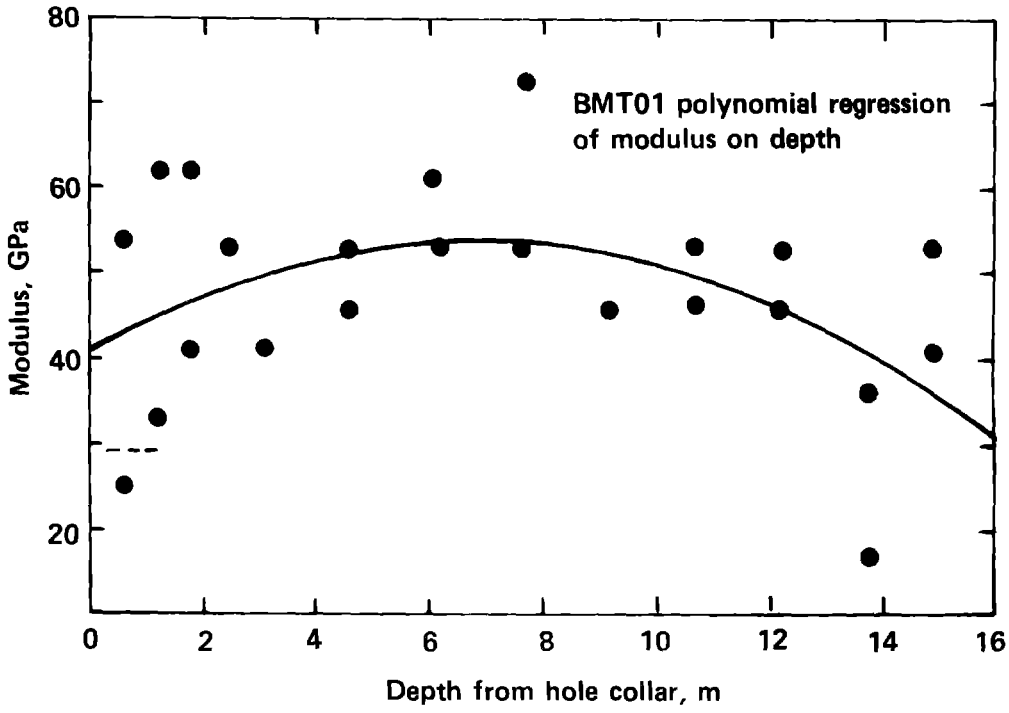

Figure 21. Polynomial regression of modulus on depth from borehole collar. Data are from both loading directions in BMT01.

modulus value vs depth from borehole collar (Fig. 22). Whereas the modulus values for vertical loading tend to cluster near 50 GPa, those associated with horizontal loading are scattered above and below this value. No root cause has been found for the roughly sinusoidal pattern that is traced out by the values associated with horizontal loading.

A general linear model using distance from center as a quantitative variable and the loading directions as two qualitative variables failed to detect a distance effect or a difference in mean modulus between the two loading directions. A matched paired analysis (dropping several points with no twin) produced results consistent with the general linear model. These results indicate that the 27 data from BMT02 are best summarized by the sample mean and its standard error, which are 47.4 and 2.4 GPa, respectively.

Exploratory Borehole UG02

Exploratory borehole UG02 presented the only opportunity to measure deformability of the rock located beneath the SFT—C. This borehole was drilled parallel to the canister drift at an angle 60° below horizontal. Measurements were made in the upper 15 m of UG02 following the 3-year episode of heating.

The presence of zones of intense fracturing near the borehole collar and at depths of 12.3 to 15 m (Wilder et al., 1982) produced a distribution of modulus with depth that is fairly symmetric about the borehole "center," where jointing was sparse. Given this symmetry, we developed a general linear model for modulus as a function of distance from borehole center and loading direction. When no loading direction effect was detected, the data were pooled, giving a slope of −7.8 GPa/m with an intercept (at borehole center) of 76 GPa (Fig. 23). While the intercept term is large in comparison with the other data sets and is near the cut-off of 85 GPa, it appears to be consistent with the general trend of the data from this borehole. The residual standard error for the UG02 data is about 10 GPa, which is similar to the other boreholes.

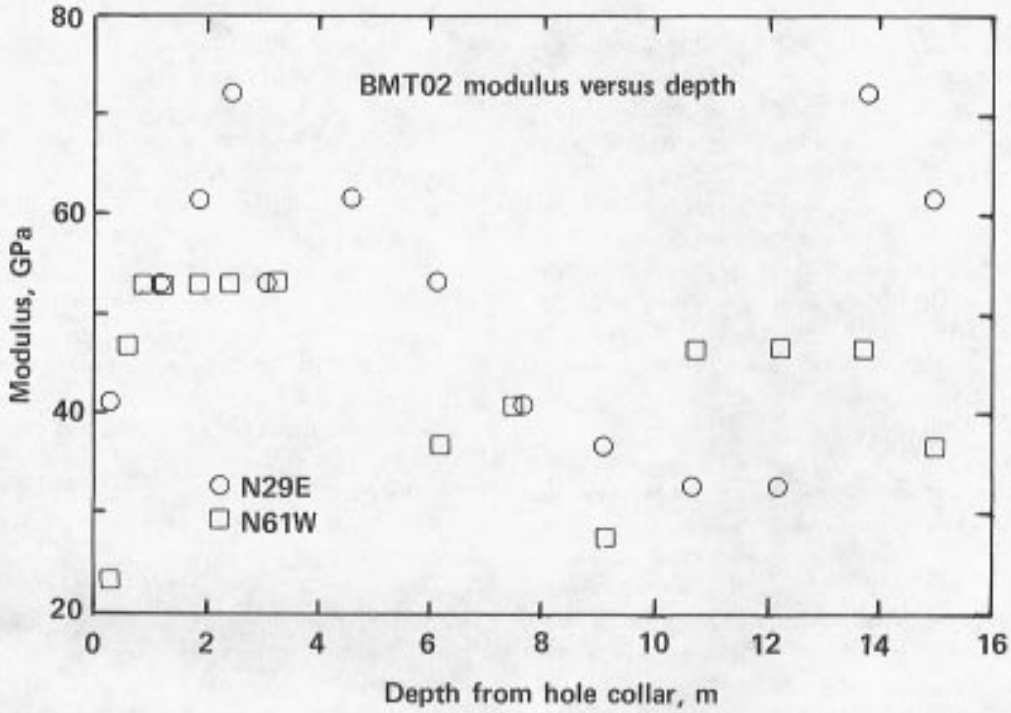

Figure 22. Relationship between borehole modulus value and distance from borehole collar for borehole BMT02.

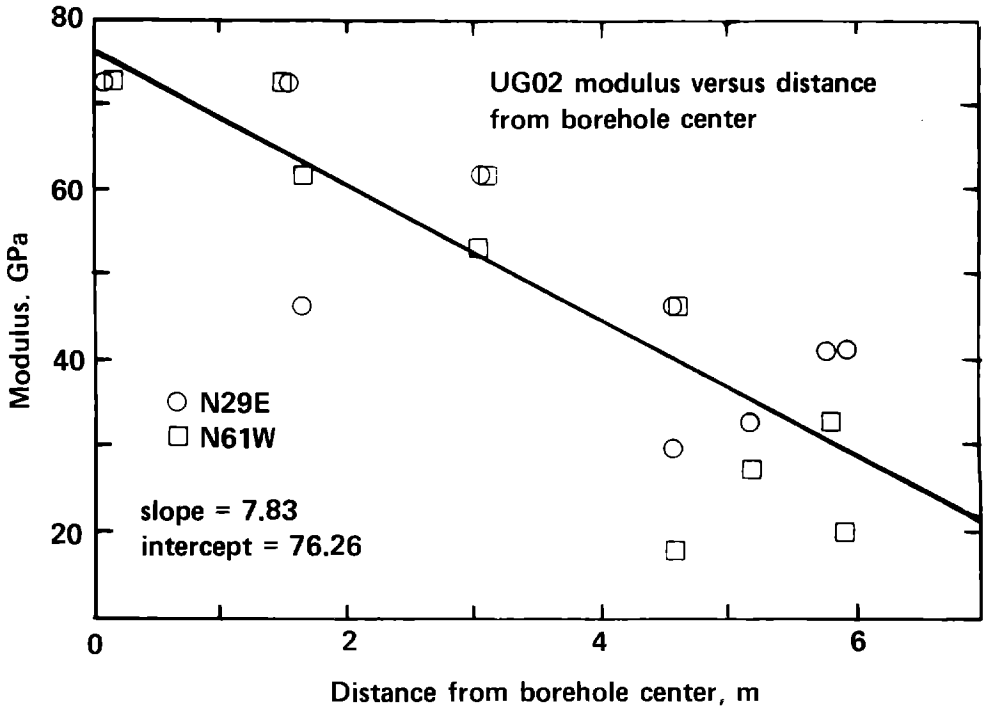

Figure 23. Relationship between borehole modulus value and distance from borehole center for exploratory borehole UG02.

Conclusions

A total of 212 deformation modulus measurements were made in nine borehole segments using a commercially available Goodman NX borehole jack. These were analyzed together with the results of 64 measurements obtained by Heuze et al. (1981) before heating began at the SFT—C. Although the study was completed before a suggested method (Heuze, 1984) for such testing was proposed, the study was in accord with the subsequent guidelines of the suggested method. The method of screening the data for full platen seating, which is proposed in the guideline, was not applied. Our observations include:

1. A simple screening technique based on the maximum of the observed laboratory modulus values eliminates measurements that are outliers in both an engineering and statistical sense. A proposed screen based on full platen seating fails to eliminate physically implausible values. The cause of these extreme values is presently unknown.

2. A statistically significant anisotropy in the deformation modulus was observed in three of four pre- and post-heating data sets. The effect was for the modulus to be about 10 GPa less under vertical loading than under horizontal loading in the preheating data set and about 10 GPa greater in the post-heating data set. Anisotropy was not found to be significant in the rock outside the SFT—C excavations, suggesting that stress changes and excavation-induced damage may be responsible for the anisotropy.

3. Currently available data indicate that moderate heating (~10°C above ambient, or 30 to 35°C) for a 3-year period resulted in a statistically significant increase in the deformation modulus measured under vertical loading. The deformation modulus under horizontal loading showed only marginal changes following heating. These changes in modulus are believed to result from changes in the stress regime that were produced by the heating.

4. An apparent reduction in deformation modulus was evident in data obtained in two boreholes (NHH10A and SHH05A) located 0.76 m radially outward from electrical heat sources. Rock temperatures in this region were near 60°C for about 3 years before modulus testing. The proximity of borehole NHH10A to a fault zone may be an additional cause of the lower modulus values.

5. We believe that the drill-and-blast technique used to excavate the underground openings and the commensurate changes in stress field

tended to decrease the deformation modulus near the surfaces of the excavations. This trend was not distinguishable in all borehole segments but was found to be statistically significant.

6. The effect in item 5 is sometimes masked by decreases in modulus near geologic features such as faults, shears, and zones of intense jointing. This effect was most pronounced in borehole MBI14N where the effect noted in item 5 is reversed.

Since the data set is highly variable, a reasonable approach may be to ignore the observed spacial variations and to use a range of deformation modulus values in calculations of the mechanical and thermomechanical response of the SFT—C. Where one is constrained to a very simple treatment of deformability, we suggest using a 10% "trimmed" mean for the entire data set (Becker and Chamber, 1984). Using this approach, a mean modulus of 37.7 GPa is calculated with 80% of the data values falling in the interval between 12 to 63 GPa.

As shown in this report, a thorough analysis of the data by orientation, region, and thermal treatment may support development of a better model of the deformation modulus. Although not all of them are *statistically* significant, the following trends are observed in the data (Appendices A and B) and may be appropriate to include in numerical models of the SFT—C based on a determination of *engineering* significance:

1. Moderately fractured rock 2 m or more from excavated surface: 40 to 55 GPa, based on post-heating measurements. This is as much as 10 GPa higher than preheating modulus values.

2. Rock within 2 m of excavated surfaces: 10 to 45 GPa.

3. Faulted, sheared, or intensely jointed rock: 5 to 20 GPa (depending on fracture intensity).

4. Rock heated to about 60°C for an extended period (about 3 years in this case): 5 to 25 GPa.

Acknowledgments

Overall guidance for this and other NNWSI projects at LLNL is provided by Dr. Lawrence Ramspott. The authors acknowledge the able assistance of Mr. Dennis Peifer in obtaining many of the reported measurements. Many helpful suggestions and improvements resulted from reviews of this text by Dr. John Franklin, Franklin Geotechnical; Drs. Francois Heuze and Robert Langland, LLNL; and Mr. Frank Shuri, Shannon and Wilson. We also extend our thanks to Dr. Steven P. Verrill who provided advice and evaluation of the statistical analyses. The raw data acquired in an earlier phase of testing were made available to us by Dr. Francois Heuze. This allowed a direct comparison of pre- and post-heating data. Saundra Gonzales and Kathryn Young typed the original manuscript.

Bibliography

Axelrod, M. C., S. P. Verrill, W. C. Patrick, and J. L. Yow, Jr., *A Monte Carlo Investigation of a Proposed Screen for NX-Borehole Jack Data*, Lawrence Livermore National Laboratory, Livermore, CA, UCRL-94087 (to be published).

Bandis, S. C., A. C. Lumsden, and N. R. Barton (1983), "Fundamentals of Rock Joint Deformation," *Int. Journal of Rock Mech. and Min. Sci. & Geomech. Abstracts* **20**, 249–268.

Becker, R. A., and J. M. Chambers (1984), *S, An Interactive Environment for Data Analysis and Graphics* (Wadsworth Advanced Book Program, Belmont, CA).

Beiriger, J. M., and W. B. Durham (1984), *SEM Studies of Stressed and Irradiated Climax Stock Quartz Monzonite*, Lawrence Livermore National Laboratory, Livermore, CA, UCID-20052.

Bradley, J. V. (1968), *Distribution-Free Statistical Tests* (Prentice Hall, Englewood Cliffs, NJ).

Butkovich, T. R. (1981), *As-Built Mechanical and Thermomechanical Calculations of a Spent-Fuel Test in Climax Stock Granite*, Lawrence Livermore National Laboratory, Livermore, CA, UCRL-53198.

Chambers, J. M., W. S. Cleveland, B. Kleiner, and P. A. Tukey (1983), *Graphical Methods for Data Analysis* (Wadsworth International Group, Belmont, CA).

Connolly, J. A. (1981), *Hydrothermal Alteration in the Climax Granite Stock at the Nevada Test Site*, Arizona State University, Tempe, AZ, M.S. Thesis.

Conover, W. J. (1980), *Practical Nonparametric Statistics* (John Wiley & Sons, New York, NY), 2nd ed.

Creveling, J. B., F. S. Shuri, K. M. Foster, and S. V. Mills (1984), *In Situ Stress Measurements at the Spent Fuel Test—Climax Facility*, Foundation Sciences, Inc., Contractor Technical Report to Lawrence Livermore National Laboratory, Livermore, CA., UCRL-15628.

Goodman, R. E. (1980), *Introduction to Rock Mechanics* (John Wiley & Sons, New York, NY).

Heuze, F. E. (1984), "Suggested Method for Estimating the *In-Situ* Modulus of Deformation of Rock Using the NX-Borehole Jack," *Geotechnical Testing Journal* **7**(4), 205–210.

Heuze, F. E., and B. Amadei (1985), "The NX-Borehole Jack: A Lesson in Trials and Errors," *Int. Journal of Rock Mech. and Min. Sci. & Geomech. Abstracts* **22**(2), 105–112.

Heuze, F. E., T. R. Butkovich, and J. C. Peterson (1981), *An Analysis of the "Mine-by" Experiment, Climax Granite, Nevada Test Site*, Lawrence Livermore National Laboratory, Livermore, CA, UCRL-53133.

Heuze, F. E., and A. Salem (1976), "Plate Bearing and Borehole Jack Tests in Rock—A Finite Element Analysis," in *Proc. 17th U.S. Symposium on Rock Mechanics, Snowbird, Utah*, pp. 4B8-1 to 4B8-6.

Maldonado, F. (1977), *Summary of Geology and Physical Properties of the Climax Stock Nevada Test Site*, U.S. Geological Survey Open File Report 77-356.

McGill, R., J. W. Tukey, and W. A. Larsen (1978), "Variations of Box Plots," *The American Statistician* **32**(1), 12–16.

Meyer, T. O., and J. R. McVey (1974), *NX Borehole Jack Modulus Determinations in Homogeneous, Isotropic, Elastic Materials*, U.S. Bureau of Mines, RI 7855.

Patrick, W. C., L. B. Ballou, T. R. Butkovich, R. C. Carlson, W. B. Durham, G. L. Hage, E. L. Majer, D. N. Montan, R. A. Nyholm, N. L. Rector, D. G. Wilder, and J. L. Yow, Jr. (1982), *Spent Fuel Test—Climax: Technical Measurements Interim Report, Fiscal Year 1981*, Lawrence Livermore National Laboratory, Livermore, CA, UCRL-53294.

Patrick, W. C., L. B. Ballou, T. R. Butkovich, R. C. Carlson, W. B. Durham, G. L. Hage, E. L. Majer, D. N. Montan, R. A. Nyholm, N. L. Rector, D. G. Wilder, and J. L. Yow, Jr. (1983), *Spent Fuel Test—Climax: Technical Measurements Interim Report, Fiscal Year 82*, Lawrence Livermore National Laboratory, Livermore, CA, UCRL-53294-82.

Pratt, H., R. Lingle, and T. Schrauf (1979), *Laboratory Measured Material Properties of Quartz Monzonite, Climax Stock, Nevada Test Site*, Terra Tek, Inc. Contractor Report, Lawrence Livermore National Laboratory, Livermore, CA, UCRL-15073.

Ramspott, L. D., L. B. Ballou, R. C. Carlson, D. N. Montan, T. R. Butkovich, J. E. Duncan, W. C. Patrick, D. G. Wilder, W. G. Brough, and M. C. Mayr (1979), *Technical Concept for a Test for Geologic Storage of Spent Reactor Fuel in the Climax Granite*, Nevada Test Site, Lawrence Livermore National Laboratory, Livermore, CA, UCRL-52796.

Ryerson, F. J., and B. J. Qualheim (1983), *Mineralogic and Petrologic Investigation of Pre-Test Core Samples from the Spent Fuel Test—Climax*, Lawrence Livermore National Laboratory, Livermore, CA, UCID-19976.

Searle, S. R. (1971), *Linear Models* (John Wiley & Sons, New York, NY).

Shuri, F. S. (1981), "Borehole Diameter as a Factor in Borehole Jack Results," in *Proc. 22nd U.S. Symposium on Rock Mechanics, Cambridge, Massachusetts* (MIT Press, Cambridge, MA), pp. 392–397.

Wilder, D. G., and J. L. Yow, Jr. (1981), *Fracture Mapping at the Spent Fuel Test—Climax*, Lawrence Livermore National Laboratory, Livermore, CA, UCRL-53201.

Wilder, D. G., J. L. Yow, Jr., and R. K. Thorpe (1982), *Core Logging for Site Investigation and Instrumentation, Spent Fuel Test—Climax*, Lawrence Livermore National Laboratory, Livermore, CA, UCID-19646.

Wilder, D. G., and J. L. Yow, Jr. (1984), *Structural Geology Report, SFT—C*, Lawrence Livermore National Laboratory, Livermore, CA, UCRL-53381.

Yow, J. L., Jr. (1985), *Field Investigation of Keyblock Stability*, Lawrence Livermore National Laboratory, Livermore, CA, UCRL-53632.

MLD/mf,js,kc

Appendix A
Rock Deformation Modulus vs Borehole Depth
(Post-Heating Measurements)

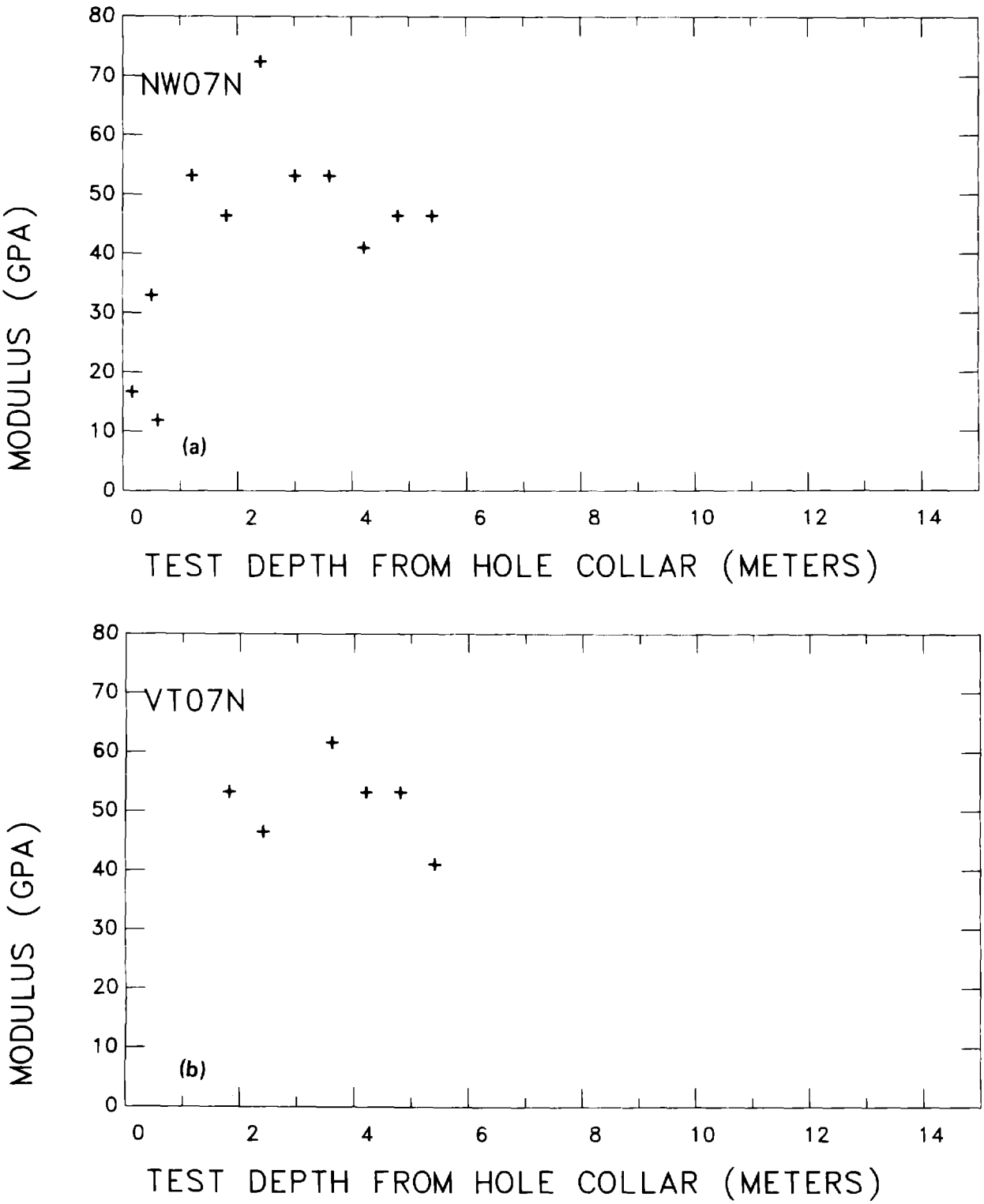

Figure A-1. Deformation modulus as a function of test depth in the north segment of borehole MBI07. Loading directions are (a) N61°W and (b) vertical.

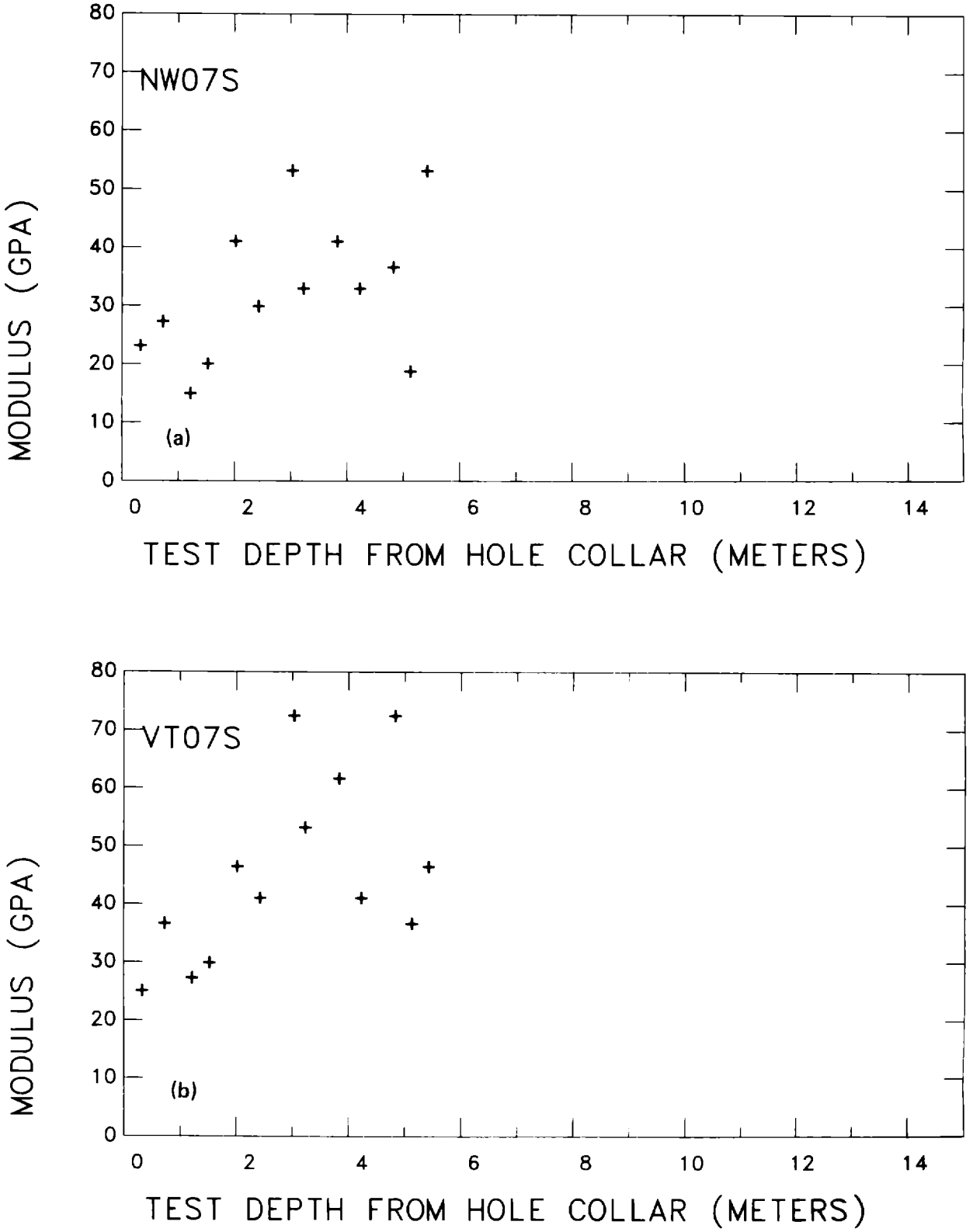

Figure A-2. Deformation modulus as a function of test depth in the south segment of borehole MBI07. Loading directions are (a) N61°W and (b) vertical.

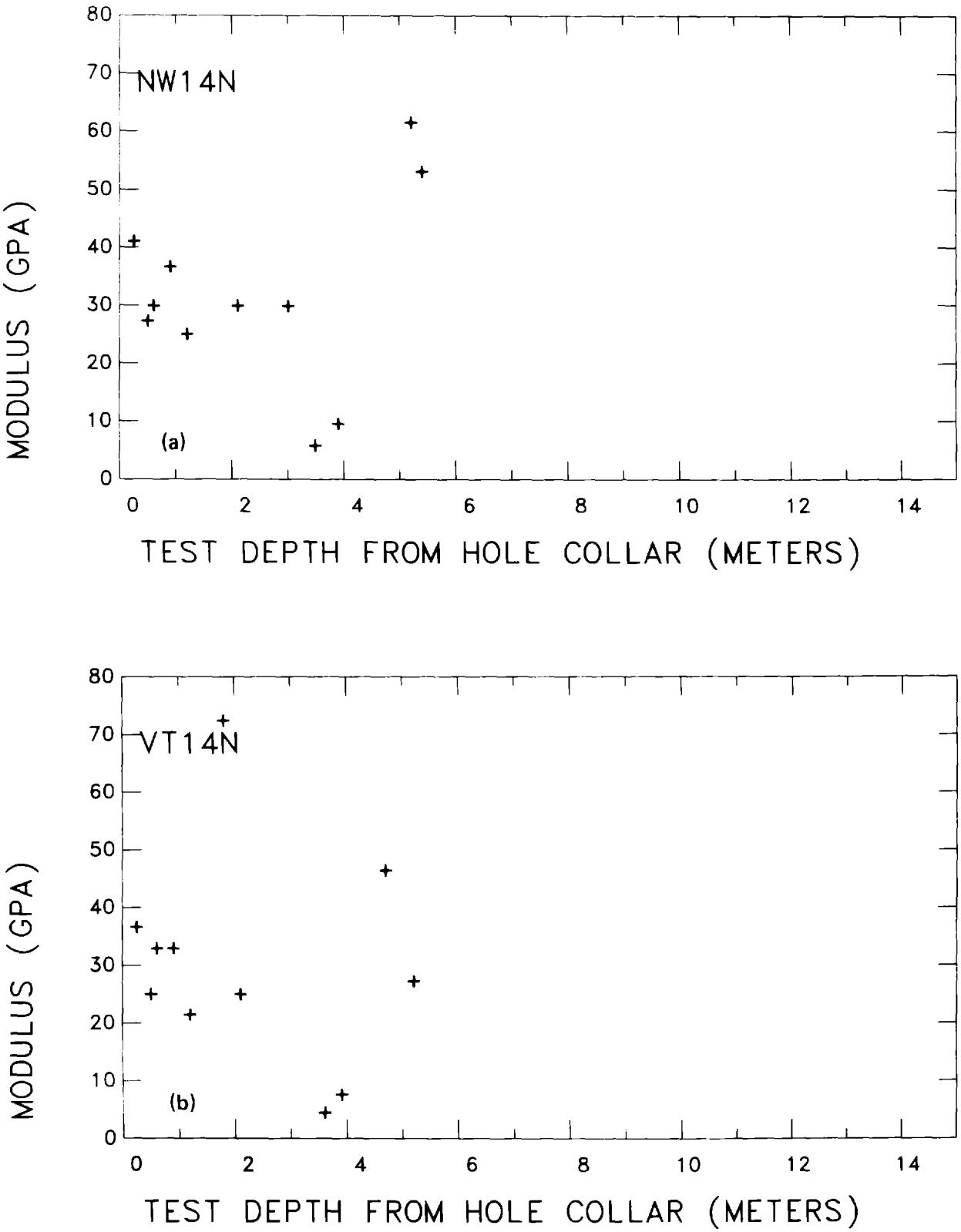

Figure A-3. Deformation modulus as a function of test depth in the north segment of borehole MBI14. Loading directions are (a) N61°W and (b) vertical.

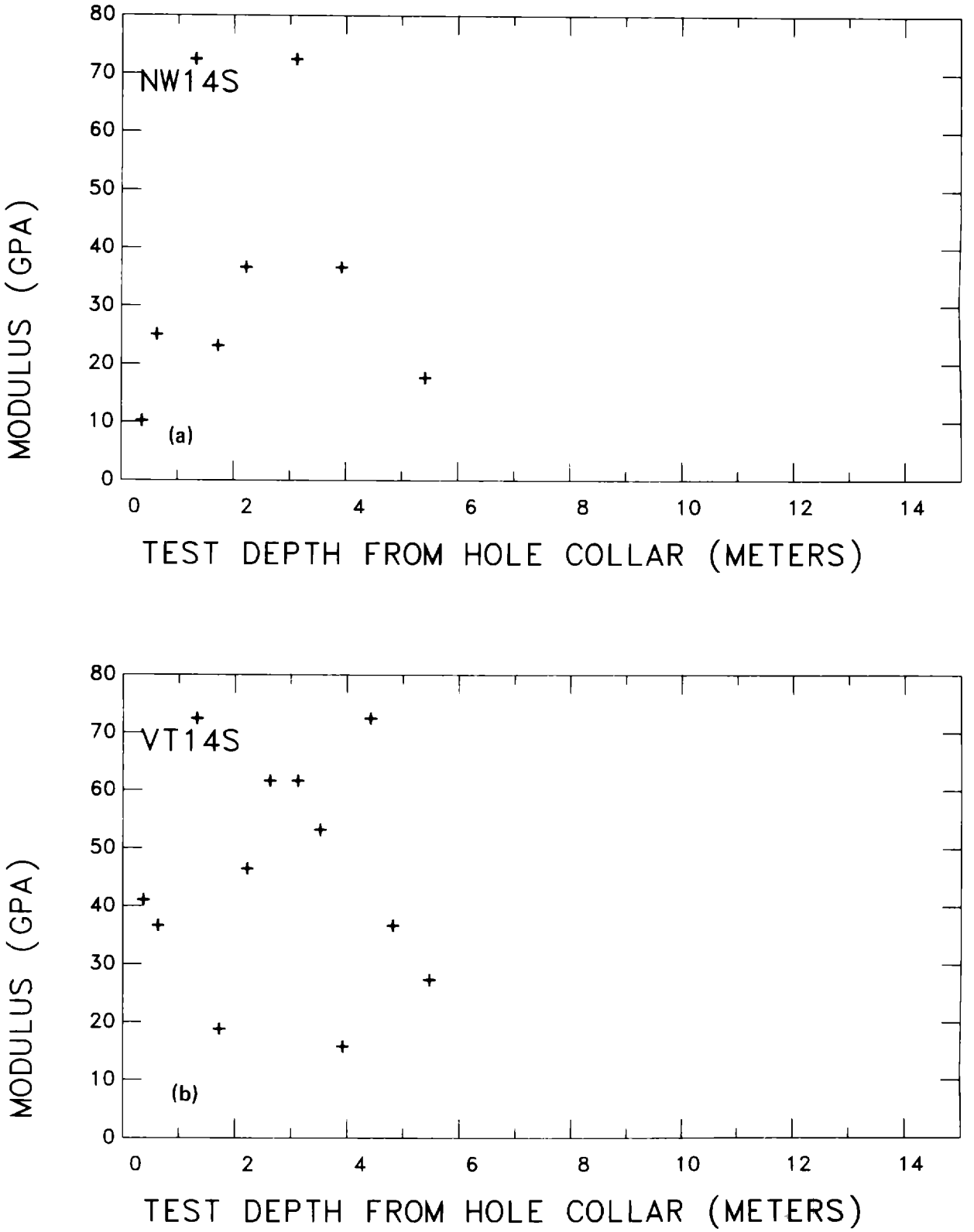

Figure A-4. Deformation modulus as a function of test depth in the south segment of borehole MBI14. Loading directions are (a) N61°W and (b) vertical.

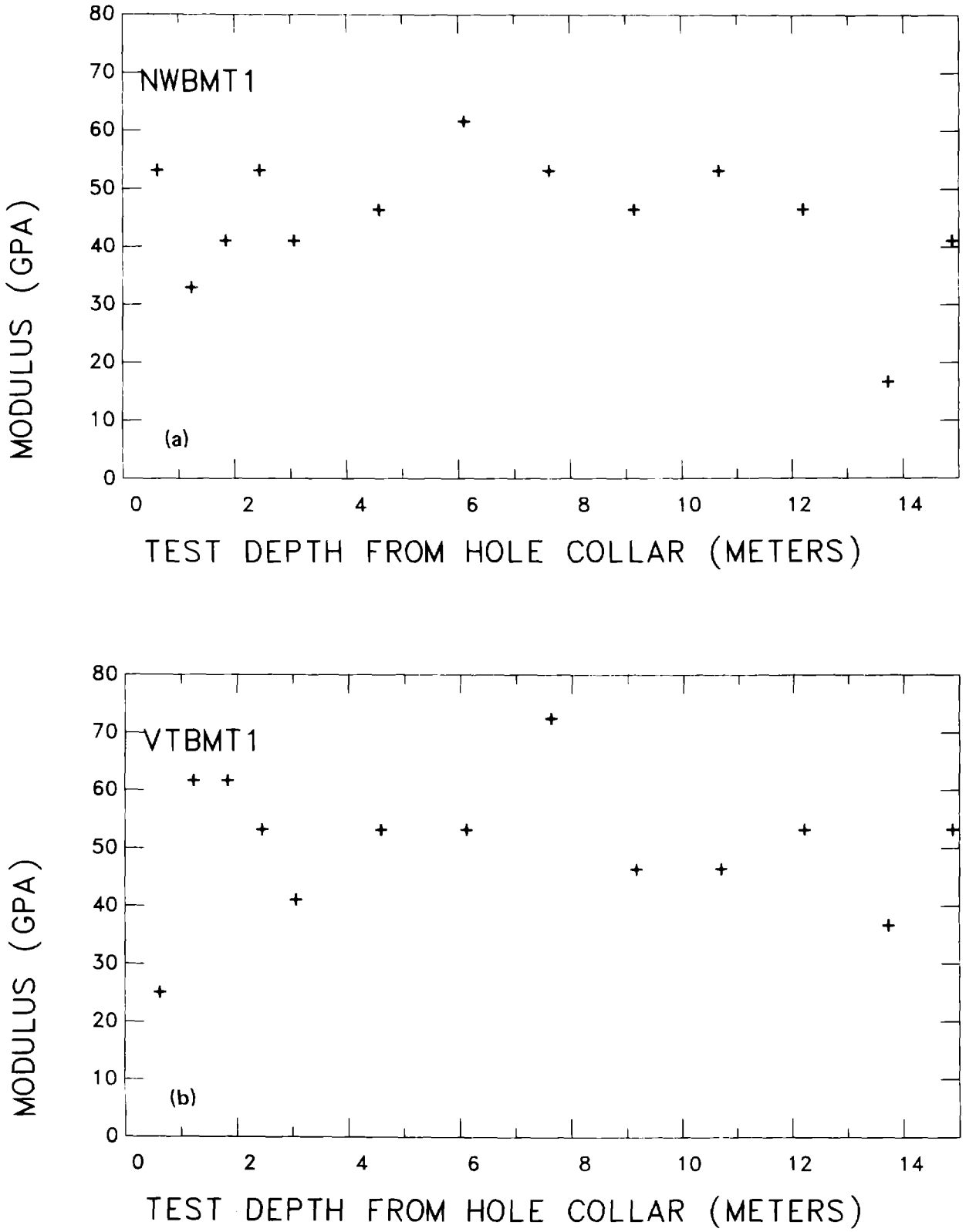

Figure A-5. Deformation modulus as a function of test depth in borehole BMT01. Loading directions are (a) N61°W and (b) vertical.

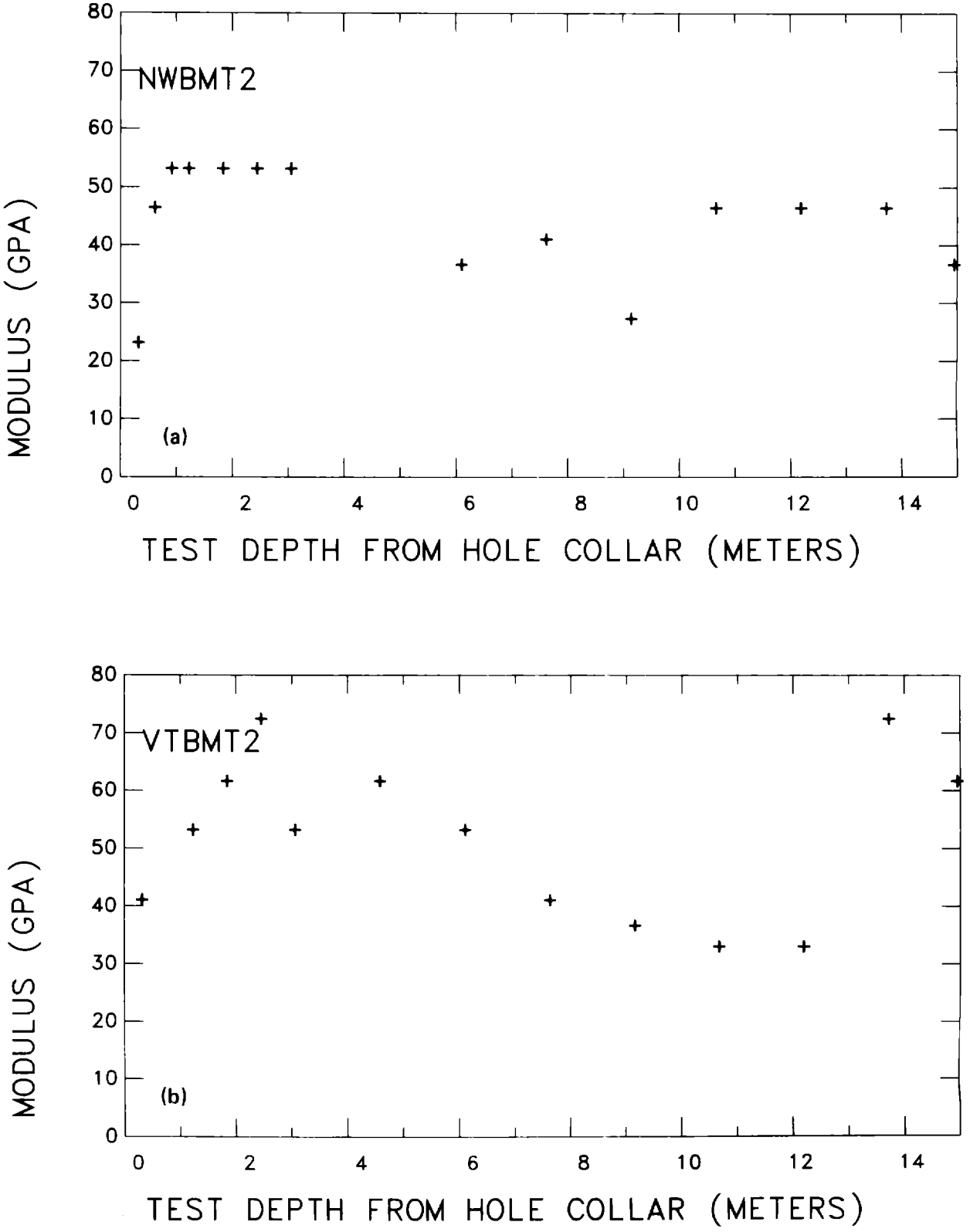

Figure A-6. Deformation modulus as a function of test depth in borehole BMT02. Loading directions are (a) N61°W and (b) vertical.

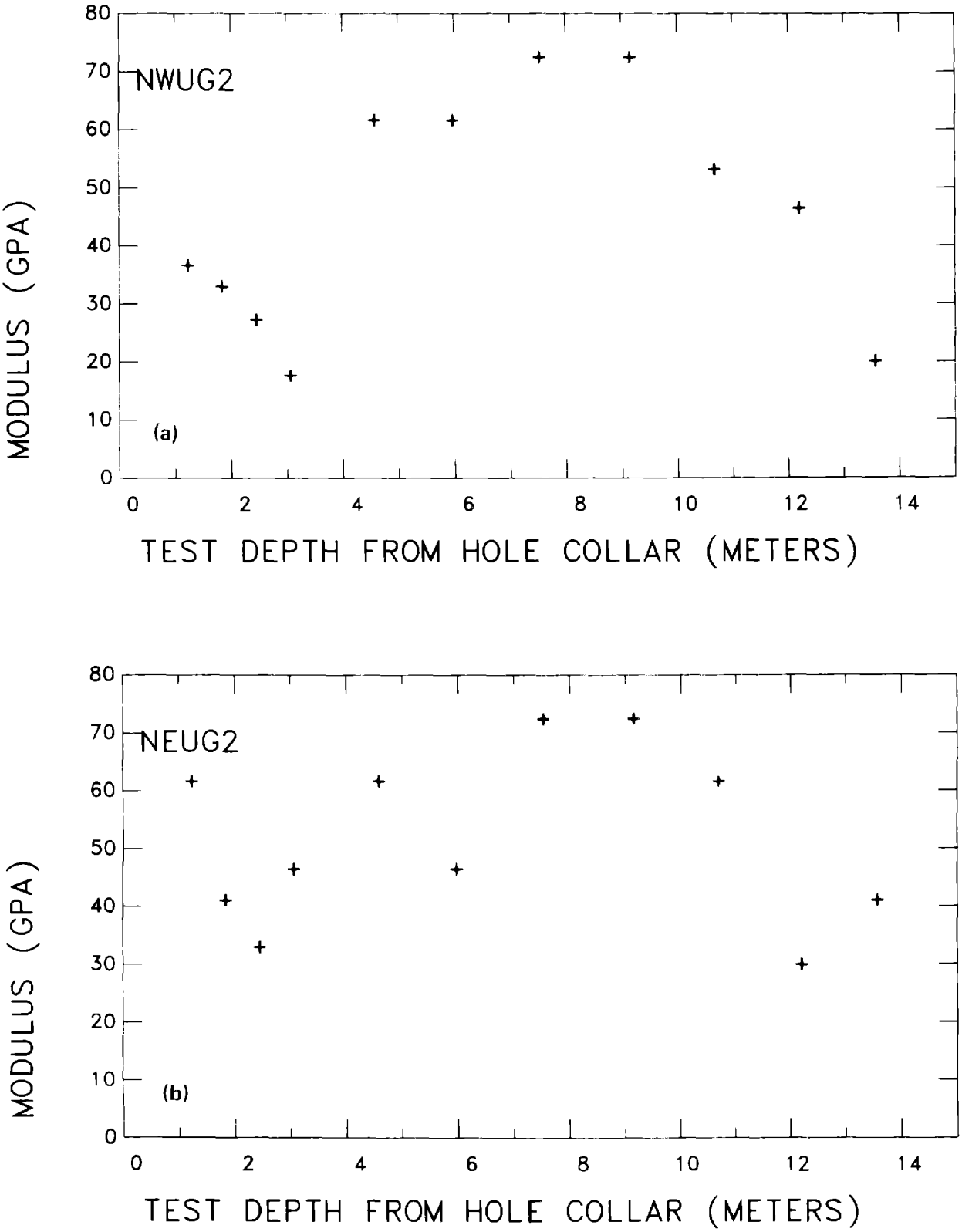

Figure A-7. Deformation modulus as a function of test depth in borehole UG02. Loading directions are (a) N61°W and (b) N29°E.

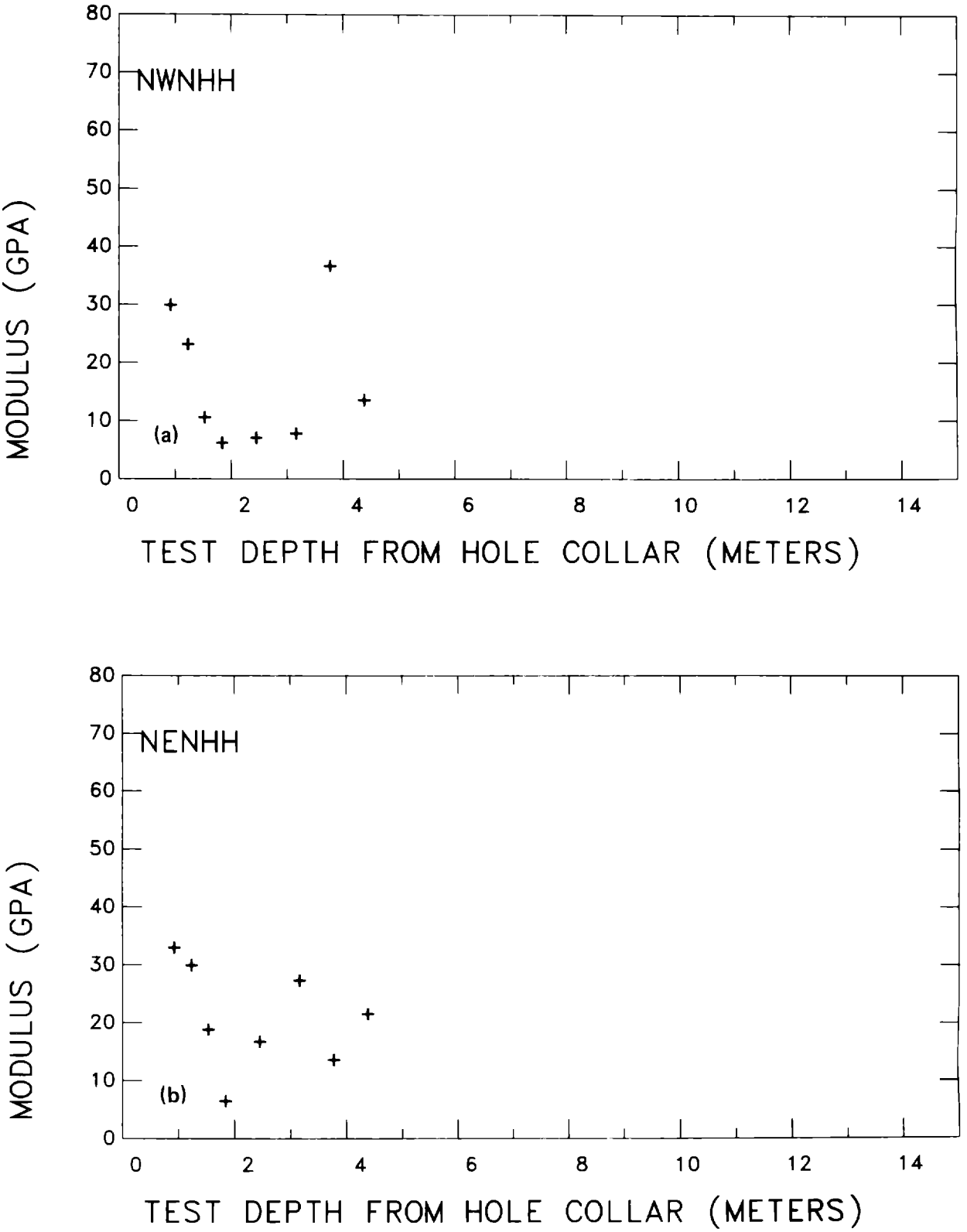

Figure A-8. Deformation modulus as a function of test depth in borehole NHH10A. Loading directions are (a) N61°W and (b) N29°E.

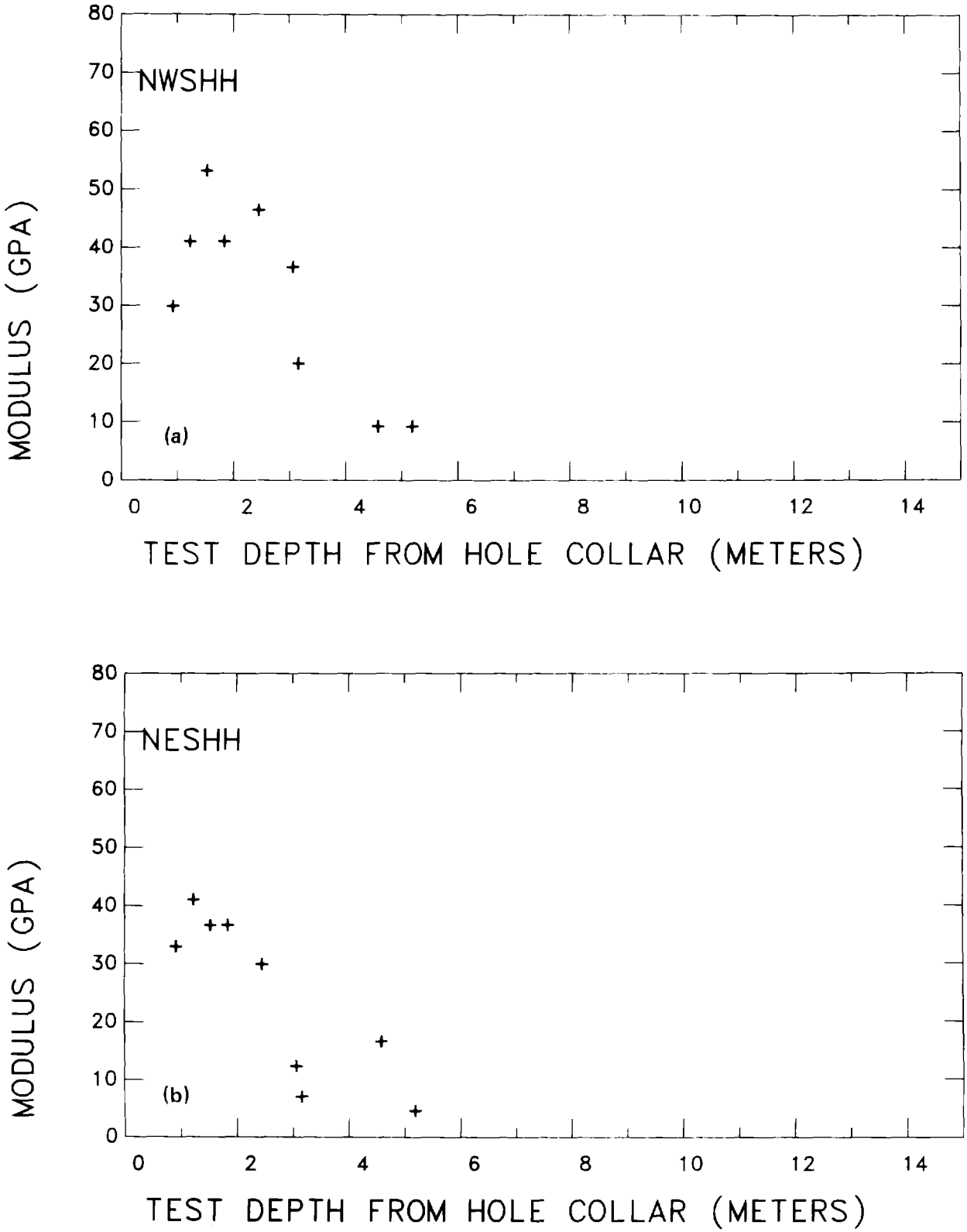

Figure A-9. Deformation modulus as a function of test depth in borehole SHH05A. Loading directions are (a) N61°W and (b) N29°E.

Appendix B
Rock Deformation Modulus vs Borehole Depth
(Recalculated Preheating Measurements of Heuze et al., 1981)

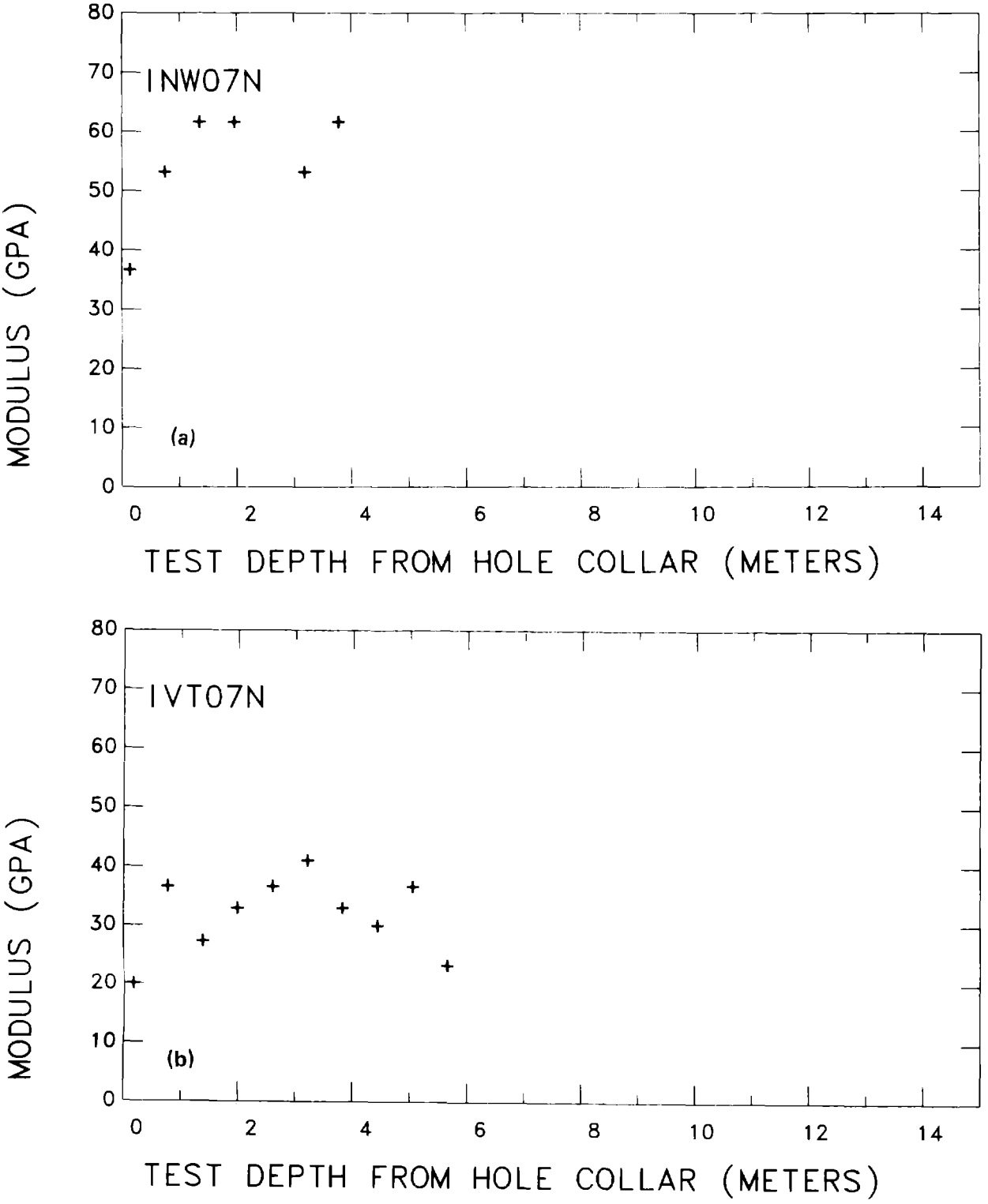

Figure B-1. Deformation modulus as a function of test depth in the north segment of borehole MBI07. Loading directions are (a) N61°W and (b) vertical. Based on raw data from Heuze et al. (1981),

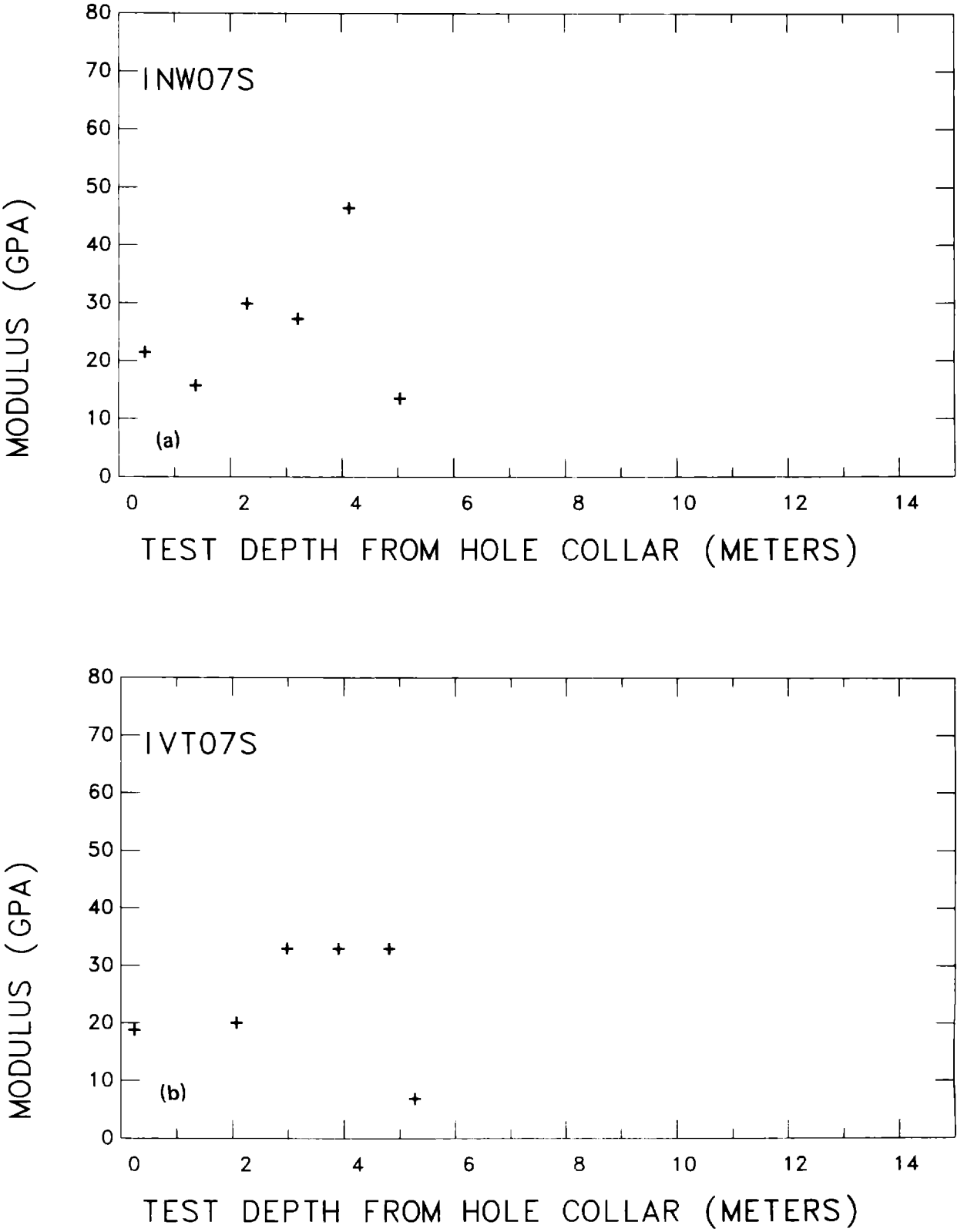

Figure B-2. Deformation modulus as a function of test depth in the south segment of borehole MBI07. Loading directions are (a) N61°W and (b) vertical. Based on raw data from Heuze et al. (1981).

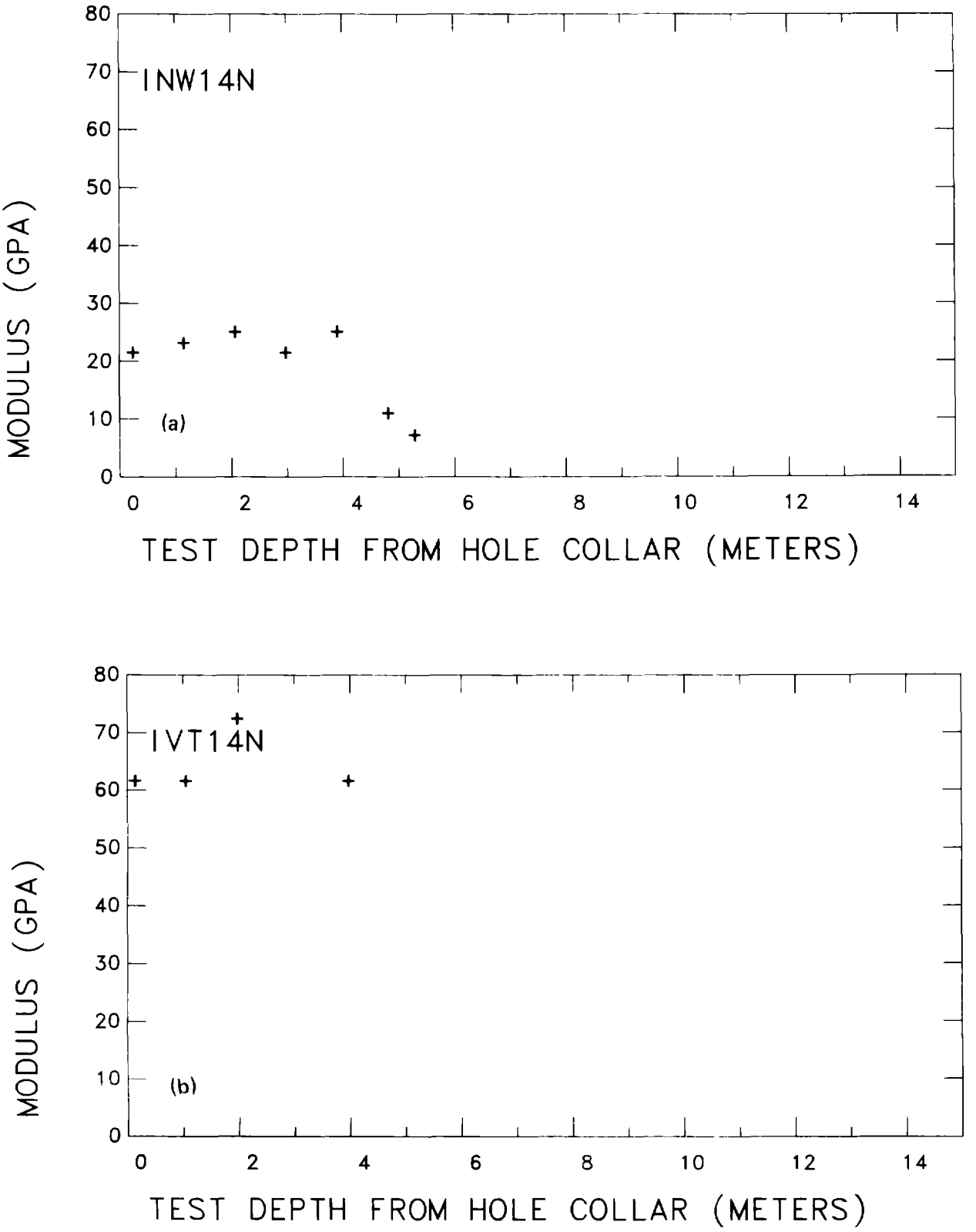

Figure B-3. Deformation modulus as a function of test depth in the north segment of borehole MBI14. Loading directions are (a) N61°W and (b) vertical. Based on raw data from Heuze et al. (1981).

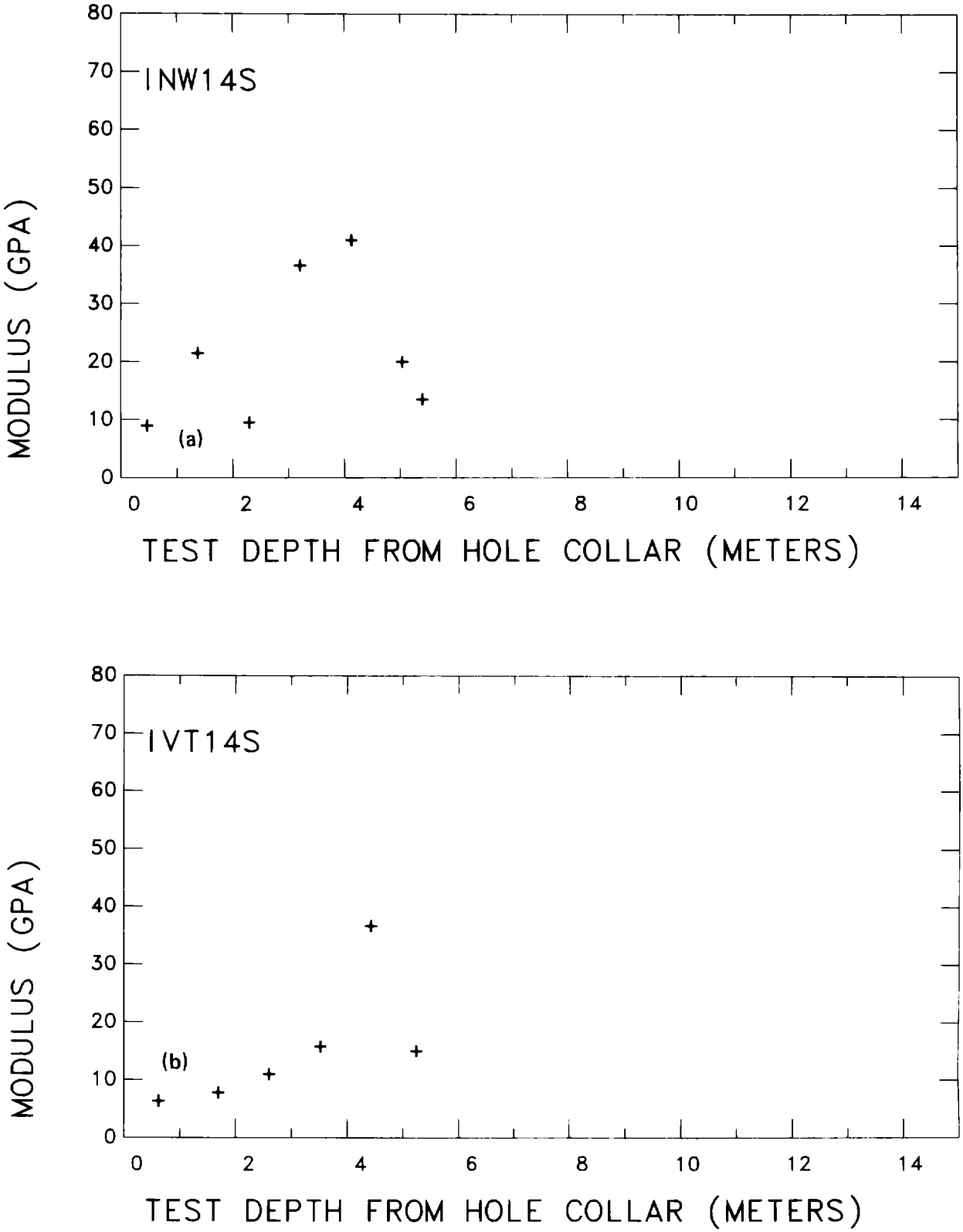

Figure B-4. Deformation modulus as a function of test depth in the south segment of borehole MBI14. Loading directions are (a) N61°W and (b) vertical. Based on raw data from Heuze et al. (1981).

Appendix C
Effects of Measurement Error on Estimates of Deformability

The calculated deformation modulus E_c [Eq. (1)] is based on the ratio of the change in hydraulic line pressure ΔQ_h to the change in borehole diameter ΔD. It is useful to know how measurement errors in these quantities affect the accuracy of this ratio. Although the ratio was determined graphically as the slope of the linear portion of the jack pressure vs displacement curve, we will assume that this is equivalent to a least squares fit of a straight line through the measurements.

The ratio can be determined from a regression of displacement on pressure. It is reasonable to select pressure as the regressor variable because the error in the pressure reading compared with the span of pressures is much smaller than the error in the displacement reading compared with the span of displacements. This leads to the following regression model:

$$y_i = \alpha + \beta x_i + \epsilon_i \qquad i = 1,2 \ldots n \quad , \tag{C-1}$$

where

y_i = observed average of near and far LVDT readings in inches,
x_i = pressure in psi,
i = index of the reading,
n = 6 (typically).

The pressure is the "design" variable in the sense that it is set by the operator. Furthermore, we assume that the set pressure value is also the true value, the pressure actually applied by the jack.

The ratio $\Delta Q_h/\Delta D$ is then the reciprocal of the estimated regression coefficient,

$$\frac{\Delta Q_h}{\Delta D} = \frac{1}{\hat{\beta}} \quad . \tag{C-2}$$

The random quantity ϵ_i in Eq. (C-1) represents the measurement error in LVDT. We can estimate the variance of $\hat{\beta}$ by

$$\mathrm{Var}(\hat{\beta}) = \frac{\sigma_\epsilon^2}{\sum_{i=1}^{n} (x_i - \bar{x})^2} \quad , \tag{C-3}$$

where σ_ϵ = standard error of the mean LVDT reading (near and far).

A typical set of pressure values is from 5000 to 10,000 psi in equal increments. A conservative value for σ_ϵ^2, the variance of the error in the mean LVDT readings, is 0.25×10^{-6} in.^{2} The variance of $\hat{\beta}$ is

$$\mathrm{Var}(\hat{\beta}) = \frac{0.25 \times 10^{-6}}{17.5 \times 10^{6}} = 0.01429 \times 10^{-12} \quad . \tag{C-4}$$

In general, the variance of a function of $\hat{\beta}$, $f(\hat{\beta})$, is given by

$$\mathrm{Var}\,[f(\hat{\beta})] = [f'(\beta)]^2 \,\mathrm{var}(\hat{\beta}) \quad .$$

For $f(\hat{\beta}) = 1/\hat{\beta}$ and β = mean of $\hat{\beta}$,

$$\mathrm{Var}\,(1/\hat{\beta}) = \frac{\mathrm{Var}(\hat{\beta})}{\beta^4} \quad . \tag{C-5}$$

A typical value for the so-called "true" modulus E_t is 5.060×10^6psi (34.9 GPa), which corresponds to a calculated modulus $E_c = 2.484 \times 10^6$ psi. This in turn corresponds to $\Delta Q_h/\Delta D = 0.72 \times 10^6$ psi/in., or $\beta = 1.3889 \times 10^{-6}$ in./psi. Using these values, we get

$$\text{Var}\,\frac{1}{\hat{\beta}} = \frac{0.01429 \times 10^{-12}}{(1.3889 \times 10^{-6})^4} = 3.839 \times 10^{9}\ \text{psi/in.} \quad , \tag{C-6}$$

which corresponds to a relative standard error of 8.6% for the ratio $\Delta Q_h/\Delta D$. The variance of the calculated modulus E_c is given by

$$\text{Var}(E_c) = [(0.86)\,(0.93)\cdot D\cdot T^*]^2\ 3.839 \times 10^{9} = 45.703 \times 10^{9}\ \text{psi}^2 \quad . \tag{C-7}$$

The variance of E_t is given by

$$\text{Var}(E_t) = (0.979484 - 4.084206 \times 10^{-8}\ E_c + 5.378274 \times 10^{-13}\ E_c^2)^2 \cdot \text{Var}(E_c) \quad . \tag{C-8}$$

Using $E_c = 2.4842 \times 10^{6}$ psi, we get

$$\text{Var}\,(E_t) = (17.615)\,(45.703 \times 10^{9})\ \text{psi}^2 = 8.05 \times 10^{11}\ \text{psi}^2 \quad , \tag{C-9}$$

which is equivalent to a standard error of 6.2 GPa.

The use of the reciprocal introduces a statistical bias in the estimate of $\Delta Q_h/\Delta D$ because the mean of the reciprocal is not exactly equal to the reciprocal of the mean. The bias can be calculated by the formula

$$E\,[f(\hat{\beta})] \approx f(\beta) + \frac{1}{2}\,f''(\hat{\beta}) \cdot \text{var}(\hat{\beta}) \quad , \tag{C-10}$$

where $f(\hat{\beta}) = 1/\hat{\beta}$ and $\beta = E(\hat{\beta})$. The bias is given by

$$E(1/\hat{\beta}) - 1/\beta = 1/\beta^3\ \text{Var}(\hat{\beta}) = \frac{0.01429 \times 10^{-12}}{(1.3889 \times 10^{-6})^3} = 5.334 \times 10^{3}\ \text{psi/in.} \quad . \tag{C-11}$$

The bias due to the reciprocal is extremely small and can be neglected.

Thus, if the slopes obtained "by hand" from the graphs are essentially the same as the slopes obtained from regression analysis, the errors in LVDT values are on the order of 6 GPa. This is about one-half the residual standard error of 10 to 13 GPa that was obtained in fitting the statistical models presented in "Results and Discussion."